Organic & Biomolecular Chemistry

ROYAL SOCIETY OF CHEMISTRY

PAPER

View Article Online
View Journal | View Issue

Cite this: *Org. Biomol. Chem.*, 2024, **22**, 2027

π-Expanded azaullazines: synthesis of quinolino-azaullazines by Povarov reaction and cycloisomerisation†

Jonas Polkaehn,[a] Richard Thom,[a] Peter Ehlers,[a] Alexander Villinger[a] and Peter Langer *[a,b]

Received 17th January 2024,
Accepted 2nd February 2024

DOI: 10.1039/d4ob00091a

rsc.li/obc

Doping and extension of polycyclic aromatic hydrocarbons (PAHs) by simple and efficient synthetic methods is of increased demand for the development of novel and improved organic electronics. Diarylindolizino[6,5,4,3-*ija*]quinolino[2,3-*c*][1,6]naphthyridines (quinolino-azaullazines) were prepared by combination of Pd catalyzed cross-coupling with Povarov and cycloisomerisation reactions. The products contain an electron-rich ullazine and an electron-poor quinoline moiety and show intramolecular charge transfer properties that can be tuned by the substitution pattern. The optical properties were studied experimentally and further elaborated by (TD)DFT calculations.

Introduction

Indolizino[6,5,4,3-*ija*]quinolines (ullazines), first synthesized and studied by Balli *et al.* in 1983,[1] are of considerable current interest in the field of materials science, due to their application as organic light emitting diodes (OLEDs), organic field-effect transistors (OFETs) or dye-sensitized solar cells (DSSC).[2,3] Due to the electronic influence of the pyrrole moiety, ullazines represent electron-rich molecules that exhibit strong intramolecular charge transfer (ICT).[2] Several synthetic methods have been developed in recent decades to further modify the properties of ullazines. Various approaches are based on the modification of the ullazine core structure by doping with heteroatoms.[4,5] Other methods are focused on the variation of the substitution pattern and substituents.[6] Furthermore, the expansion of the π-system represents a promising approach to modify the optical and electronic properties of ullazines (Fig. 1).[7,8–15] In 2012, Ren and co-workers published the synthesis of dibenzoullazines by Friedel–Crafts arylation of aryl triazenes.[8] Similarly substituted dibenzoullazines were obtained by Pd-catalyzed twofold annulation reactions of arynes in 2021.[9] Müllen *et al.* and Nozaki *et al.* reported in 2015 the synthesis of π-extended ullazines by cycloaddition of polycyclic aromatic azomethine ylides.[10,11] The most common strategy for the synthesis of π-expanded ullazines is based on employment of azomethine ylides. Other examples have been reported by Feng *et al.*,[12] Nozaki *et al.*[13] and Stępień *et al.*[14] Moreover, Stępień *et al.* were able to synthesize such compounds by cyclodehydrohalogenation of α,α-disubstituted *N*-arylpyrroles.[14] Using photochemical cyclodehydrochlorination, Morin and coworkers synthesized π-extended ullazines annulated to two pyridine or two thiophene moieties in 3,4- and 8,9-position.[15]

A well-known methodology for the preparation of polycyclic aromatic heterocycles is the Povarov reaction, a hetero-Diels–Alder reaction that was developed in 1967.[16] In recent years, there has been renewed interest in this methodology.[17] In 2020, Jana *et al.* reported the application of the Povarov reaction for the synthesis of dibenzo[*a*,*c*]acridines from 2′-alkynylbiaryl-2-carbaldehydes using catalytic amounts of $FeCl_3$ (Fig. 2).[18] Recently, we reported the synthesis of benzo[*j*]naphtho[2,1,8-*def*][2,7]phenanthrolines, π-expanded azapyrenes, by combination of a Povarov with a cycloisomerization reaction.[19] Herein, we wish to report the synthesis of what are, to the best of our knowledge, hitherto unknown diarylindolizino[6,5,4,3-*ija*]quinolino[2,3-*c*][1,6]naphthyridines by combination of Povarov and cycloisomerization reactions. The incorporation of an electron-rich, five-membered pyrrole ring will alter the optoelectronic properties of this polycyclic aromatic scaffold and will be studied in detail by experimental and theoretical methods. In addition, the non-symmetric π-expansion of azaullazines will be studied in comparison to previously reported symmetric dibenzoullazines.

[a]*Institute of Chemistry, University Rostock, Albert-Einstein-Str. 3a, 18059 Rostock, Germany. E-mail: peter.langer@uni-rostock.de; Fax: +49 381 498 6412; Tel: +49 381 498 6410*

[b]*Leibniz Institute for Catalysis (LIKAT) at the University Rostock, Albert-Einstein-Str. 29a, 18059 Rostock, Germany*

† Electronic supplementary information (ESI) available: Single crystal X-ray data, ^{1}H-, ^{19}F, ^{13}C-NMR spectra of isolated compounds; computational details. CCDC 2292306. For ESI and crystallographic data in CIF or other electronic format see DOI: https://doi.org/10.1039/d4ob00091a

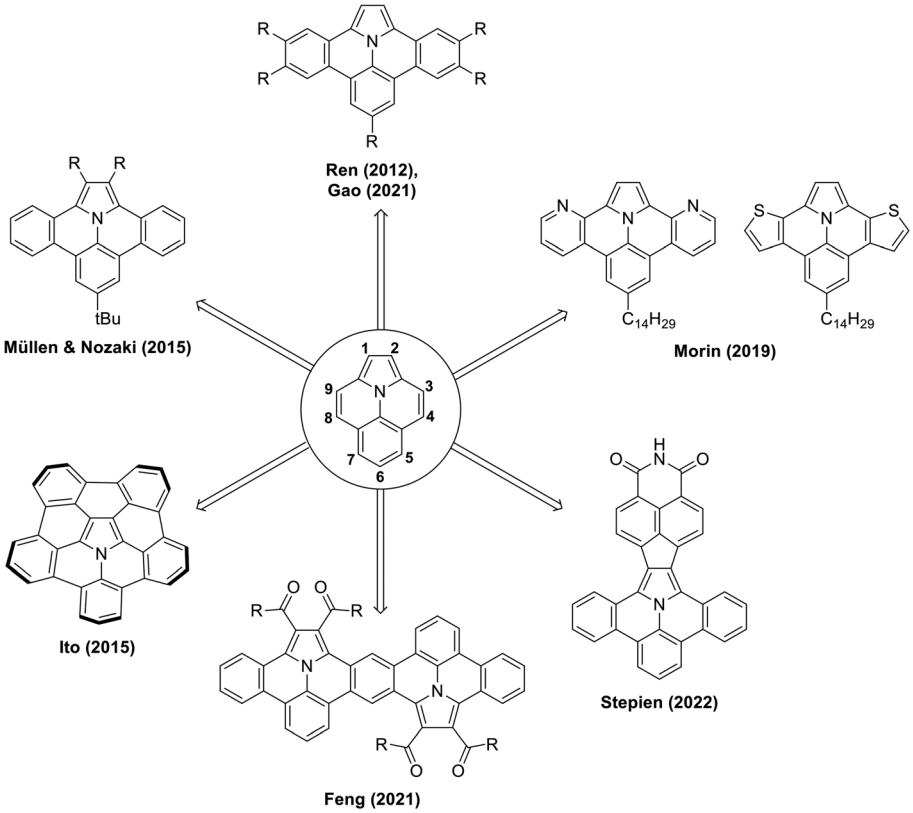

Fig. 1 Examples of π-expanded ullazines.

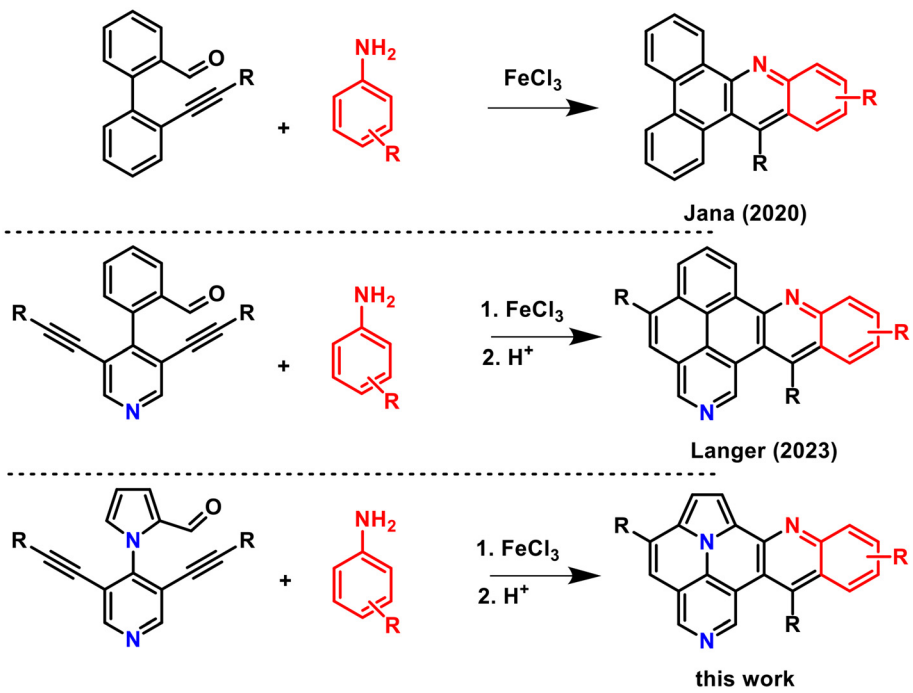

Fig. 2 Recent examples of Povarov reactions.

Synthesis

Vilsmeier–Haack reaction of 3,5-dibromo-4-(1*H*-pyrrol-1-yl)pyridine (**1**)[5] afforded formylated products **2a** and **2b** in 33% and 62% isolated yields, respectively (Scheme 1). During the optimization of, different reaction conditions were tested (ESI, Table 1†). It turned out that the use of 2 eq. of $POCl_3$ in DMF at 100 °C and 3 h reaction time provided the best results. The regiosiomeric mixture could be readily separated by column chromatography. Therefore, although the desired regioisomer **2a** was formed as the minor product, the method was useful in our hands to prepare sufficient material to continue the synthesis.

With **2a** in hand, an optimization of the following double Sonogashira reaction was carried out for the synthesis of **3a** (ESI, Table 2†). The best yields were obtained by using $PdCl_2(PPh_3)_2$ (0.05 eq.) as the catalyst and cataCXium A (0.1 eq.) as the ligand. These conditions were then applied for the synthesis of Sonogashira products **3a–e** were obtained in moderate to very good yields (Scheme 2).

Subsequently, the Povarov reaction of **3a** with aniline was studied to give product **4** (Table 1). We initially applied the conditions reported by Jana *et al.* ($FeCl_3$, toluene, 100 °C) and obtained **4** in a very good yield of 86%.[18] In contrast, employment of $In(OTf)_3$ gave a diminished yield (41%) and Brønsted acids were completely ineffective for this reaction.

Subsequently, we studied the cycloisomerization of **4** to give quinolino-azaullazine **5a** and tested *p*-toluenesulfonic acid (*p*-TsOH) and methanesulfonic acid (MsOH) which were previously used for related reactions (Table 2).[5,20] Employment of *p*-TsOH gave a better yield of 62% as compared to MsOH under the same concentration of acid (30 eq.). Reducing the amount of acid from 30 to 20 equivalents resulted in a slightly improved yield of 67%, further reduction to 10 equivalents resulted in diminished yield (43%). During the purification of **4**, we observed an alkyne-carbonyl-metathesis (ACM) reaction as competitive side reaction of the Povorav reaction.[21] Purification from this side-product was very difficult and, hence, we attempted to directly convert **3b** to **5a** in a one-pot procedure without isolation of Povarov product **4**. To our delight, this idea proved to be successful and allowed to isolate the desired quinolino-azaullazine **5a** in 47% overall yield.

Next, we were interested in the preparative scope of our methodology. Hence, the substitution pattern of the arylacety-

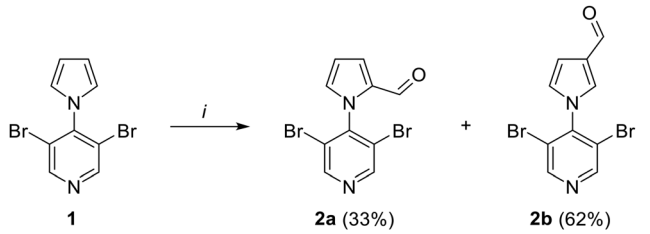

Scheme 1 Synthesis of **2a** and **2b**; (i): $POCl_3$ (2.0 eq.), DMF, 100 °C, 3 h.

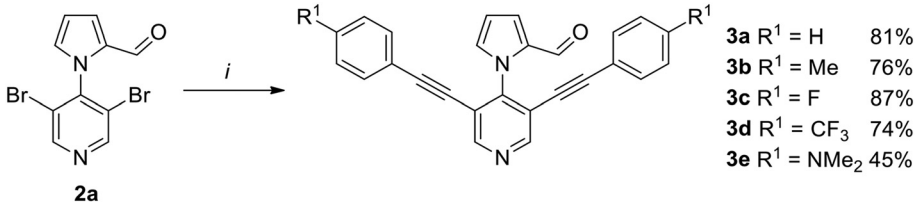

Scheme 2 Synthesis of **3a–e**; (i): alkyne (3 eq.), $PdCl_2(PPh_3)_2$ (0.05 eq.), cataCXium A (0.1 eq.), CuI (0.05 eq.), HN^iPr_2, 1,4-dioxane, 90 °C, 24 h.

Table 1 Optimization of the synthesis of **4**

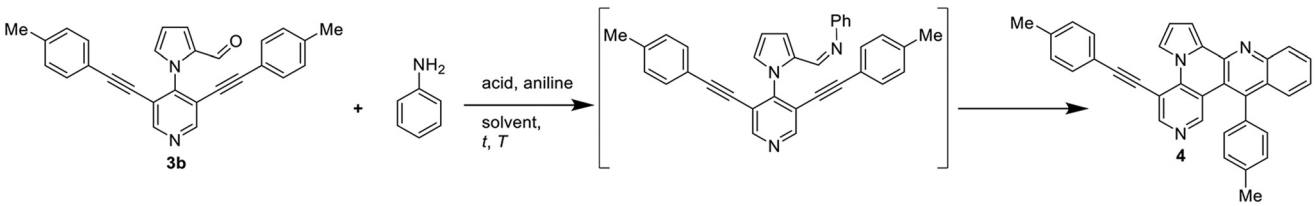

Entry	Reagent (eq.)	Eq. aniline	Solvent	*T* [°C]	*t* [h]	Yield[a] [%]
1[b]	**$FeCl_3$ (0.1)**	**1.2**	**Toluene**	**100**	**2**	**86**
2	$In(OTf)_3$ (0.1)	1.2	Toluene	100	3	41
3	*p*-TsOH·H_2O (0.1)	1.2	Toluene	100	3	0
4	TfOH (0.1)	1.2	Toluene	100	24	0

[a] Isolated yield. [b] Conditions of Jana *et al.*[18]

Table 2 Optimization of the synthesis of **5a**

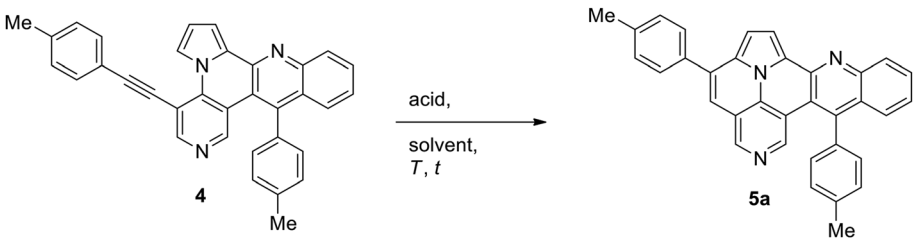

Entry	Reagent (eq.)	Solvent	T [°C]	t [h]	Yield[a] [%]
1	*p*-TsOH·H_2O (30)	Xylene[b]	120	6	62
2	MsOH (30)	Xylene[b]	120	6	40
3	***p*-TsOH·H_2O (20)**	**Xylene[b]**	**120**	**6**	**67**
4	*p*-TsOH·H_2O (10)	Xylene[b]	120	6	43

[a] Isolated yield. [b] Isomeric mixture.

lene and of the aniline were varied (Table 3). The reaction of **3a–e** with various anilines afforded quinolino-azaullazines **5a–f,h–l** in mostly moderate to good yields. All yields refer to a one-pot process in which four new bonds were formed in a single step without the need of purification of intermediates (formation of the imine, Povarov reaction and cycloisomerization). The reaction of aniline with **3e**, containing the strongly electron donating NMe_2 substituent, gave product **5c** in a reduced yield of 21%. However, the reaction of **3e** with reaction with 4-fluoroaniline afforded the corresponding product **5k** in a better yield of 39%. The best yield (product **5l**, 65%) was observed for the reaction of **3c**, containing an electron-withdrawing fluoride substituent, with 4-fluoroaniline. Heterocyclic 4-aminopyridine did not undergo a Povarov reaction (**5g**). The use of 1-naphthylamine provided product **5h** in good yield. Comparison of the yields of products derived from different substituents attached to the alkyne (**5a**, **5j** and **5k**) did not reveal a significant influence of the substitution pattern, except from the fact that the reaction of 4-fluoroaniline with **3d**, containing a trifluoromethyl group, proved to be entirely unsuccessful. In summary, the aniline has a higher influence on the yield that the substituent attached to the alkyne.

The structure of **5d** was independently confirmed by X-ray crystal structure analysis (Fig. 3). Crystallization was carried out in a mixture of heptane and dichloromethane (DCM). For a better visualization, the co-crystallized DCM has been removed. Both *p*-tolyl residues are twisted out of plane of the core structure by dihedral angles of 45° and 78°. Moreover, the crystal lattice shows a slipped antiparallel π–π-stacking with a spacing of 3.44 Å and 3.41 Å between the core structures, respectively.

Physical properties

The photophysical properties of selected derivatives were determined by steady-state absorption and photoluminescence spectra (PL) (Fig. 4). The UV/VIS-spectra indicate strong absorption bands at approx. 250–300 nm and weaker bands at approx. 450–500 nm for all compounds. Comparing the different aniline-derived moieties, a slight influence of the substituents is evident. Thus, **5a** and **5d** show very similar absorption values and shapes of the absorption bands while π-extended compound **5h** exhibits somewhat higher extinction coefficients. In contrast, **5c** has a visibly lower absorption intensity accompanied with loss of fine structure. Additionally, a red shift of the maxima is observed, which can be attributed to the strong donor properties of the *N*,*N*-dimethylamio unit. Compounds **5d**, **5j** and **5k** provide almost identical absorption spectra, due to the twisted orientation of the phenyl rings. Incorporation of a strong donor substituent, as present in **5k**, leads to an altered absorption spectrum as well as loss of fine structure. The redshift, on the other hand, is not as pronounced as for **5c**.

The PL-spectra, **5d**, **5j** and **5k** also show identical band structures and an emission maximum at 525 nm. Only donor-substituted derivative **5k** exhibits a red shift by 14 nm as compared to the other derivatives. Similar to the absorption properties, variation of the substituents directly attached to the heterocyclic core structure alters the PL-spectra to a greater extent. Compared to unsubstituted derivative **5a** (λ_{em} = 515 nm), *N*,*N*-dimethylamino-substituted compound **5c** shows the strongest red shift (λ_{em} = 539 nm), followed by fluorine-substituted **5d** (λ_{em} = 525 nm), while the strongest blue shift occurs for **5h** (λ_{em} = 505 nm).

Most compounds show quantum yields between 19% and 28%. The highest value was determined for **5h** (Φ = 0.35). In contrast, the two *N*,*N*-dimethylamino-compounds **5c** (Φ = 0.19) and **5k** (Φ = 0.20) show the lowest quantum yields. The spectroscopic data are presented in Table 4.

Since the absorption and emission spectra of **5c** and **5k** indicated the strongest influence of the substituents on the core structure, these compounds as well as reference compound **5a** were additionally investigated by time-dependent density functional theory (TD-DFT) calculations using

Table 3 Synthesis of **5a–m**

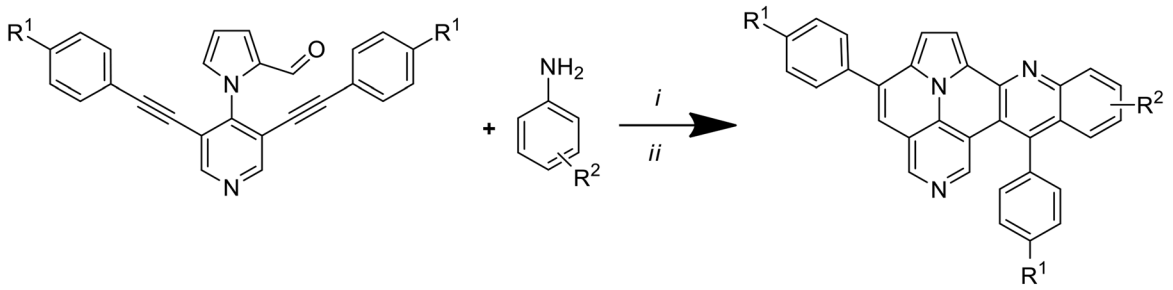

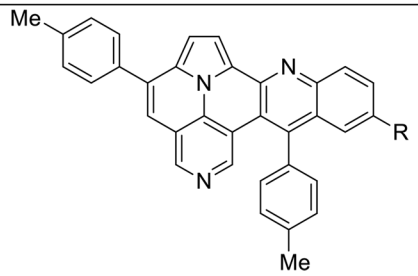

5a R = H 47 %
5b R = Me 44%
5c R = NMe_2 21%[a]
5d R = F 50%

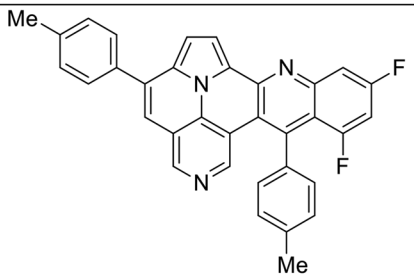

5e 46%

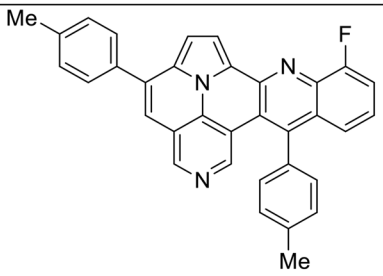

5f 41%

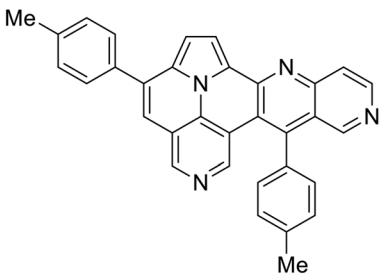

5g 0%

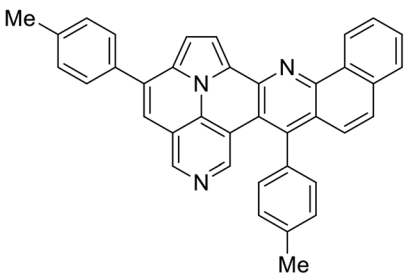

5h 46%

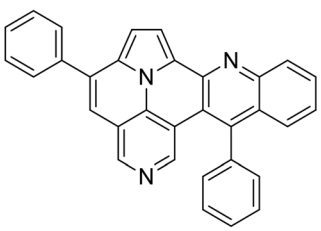

5i 32%[b]

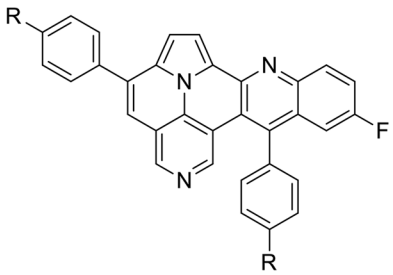

5j R = H 35%
5k R = NMe_2 39%
5l R = F 65%
5m R = CF_3 0%

(*i*): $FeCl_3$ (0.1 eq.), corresponding aniline (1.2 eq.), toluene, 100 °C, 2 h; (*ii*): *p*-TsOH·H_2O (20 eq.), xylene, 120 °C, 6 h. [a] (i): $FeCl_3$ (1.0 eq.); (ii): 20 h. [b] Longer reaction time: (i): 4 h; (ii): 20 h.

Gaussian 09 to get insight into transition characters.[23] The results show that the $S_1 \leftarrow S_0$ excitation for **5a** and **5c** is described by a HOMO → LUMO transition with high oscillator strength. The same applies to **5k**, but with additional minor contribution of HOMO−1 → LUMO and lower oscillator strength for this transition. However, the $S_2 \leftarrow S_0$ transition, which for **5k** again consisted of a HOMO → LUMO and HOMO−1 → LUMO transition, has a significantly higher oscil-

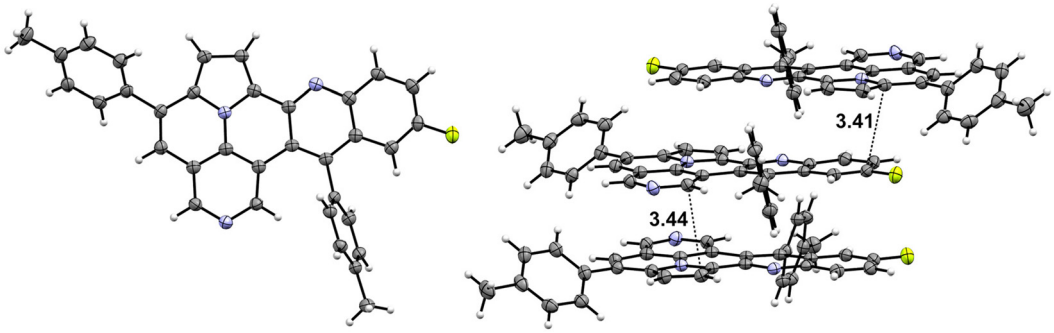

Fig. 3 X-ray structures of **5d**.

lator strength as compared to **5a** and **5c**. Hence, the orbital contribution of these transitions is reversed. In agreement with the experimental results, TD-DFT calculations reveal the greatest impact for derivative **5k**, containing a strong π-donor attached to the heterocyclic core structure.

Comparison of non-symmetric quinolino-azaullazine **5a** with symmetric dibenzoullazines of Gao and Morin and of isoelectronic quinolino-azapyrene reveal further insights into the optical properties of **5a** (Table 5).[9,15,19] Absorption and emission maxima of **5a** are both strongly, bathochromically shifted compared to all three structurally related compounds. The quantum yield of **5a** is reduced to approximately half of the value of quinolino-azapyrene, while extinction coefficients are rather similar for both compounds. A similar trend is observed for 2-aza-pyrene and 2-aza-ullazine without fused quinoline moieties.[5,20] In a smaller extend, quantum yield of **5a** is also reduced compared to symmetric dibenzoullazine reported by Gao and co-workers.[9] However, in impact on the quantum yield of **5a** by the presence of additional tolyl groups and hence increased non-radiative decay compared to dibenzoullazine can currently not ruled out.

To get an understanding of the redox properties, compound **5a** was studied by cyclic voltammetry (CV) (Fig. S1 and S2†). Compound **5a** possesses an irreversible oxidation potential at 0.72 V with an onset potential of 0.61 V, as well as a quasi-reversible oxidation potential at 1.09 V. An irreversible reduction potential was detected at −2.09 V with an onset potential of 1.90 V and a second reduction potential at 3.11 V. The HOMO energy was calculated from the onset potential and is with −5.41 eV somewhat higher than that of previously reported quinolino-azapyrene **6** which is a result of the donor-capacity of the ullazine substructure of **5a**.[19] The determined LUMO energy is −2.90 eV.

We performed density functional theory (DFT) calculations to obtain further insights into the electronic structures and transition characters. The calculations were performed for compounds **5a**, **5c**, **5i** and **5k**. Quinolino-azapyrene **6** and quinolino-ullazine **7** were additionally studied to compare the impact of different core structures (Fig. 5). The calculated HOMO–LUMO gap of the quinolino-azapyrene system is considerably larger, which is mainly due to increased HOMO energies, whereas the LUMO-energies are largely unchanged, highlighting the donating ability of the involved ullazine and azaullazine moiety. Similar HOMO–LUMO-gap energies were determined both for ullazine and azaullazine based structures **5a**, **5i** and **7**. However, an improved stabilization of both HOMO and LUMO orbitals is observed in case of azaullazines **5a** and **5i** with respect to ullazine **7**, which is obviously a result of the presence of the additional nitrogen atom. The NMe_2-groups attached to the heterocyclic core structure (**5c**) as well as the NMe_2-groups attached to the phenyl ring (**5k**) lead to reduced band gaps and elevated HOMO and LUMO energies. A more distinct effect is observed for **5c** as compared to **5k**. However, HOMO and LUMO energies are more destabilized by incorporation of one NMe_2-group directly to the core structure (**5c**) than it does for **5k** with NMe_2-groups attached to each of the two phenyl rings. Furthermore, an ICT character for **5k** can be assumed from its frontier orbitals, derived from its certain push–pull substitution pattern and its optical properties.

The potential occurrence of ICT properties was further validated by solvatochromic studies. Hence, the optical properties in solvents of different polarity were studied for NMe_2-containing compounds **5c** and **5k**, as well as for **5a** (Fig. 6). All absorption spectra show similar behavior in non-polar cyclohexane. A definite fine structure of the absorption bands, as typical for various acenes[24] and acridines,[25] can be observed for all investigated derivatives. This fine structure is lost when the polarity of the solvents increases. This indicates the presence of an ICT effect in all three derivatives **5a**,**c**,**k** and suggests that the ICT character is already present in the heterocyclic core structure, regardless of the substituent. This assumption is supported by the emission spectra, in which all compounds show two maxima and one shoulder at higher wavelength in cyclohexane. In more polar solvents, the emissions appear broadened with a single maximum. Furthermore, a bathochromic shift of emission maxima is visible for these solvents. The shift is ~40 nm for **5a** and for

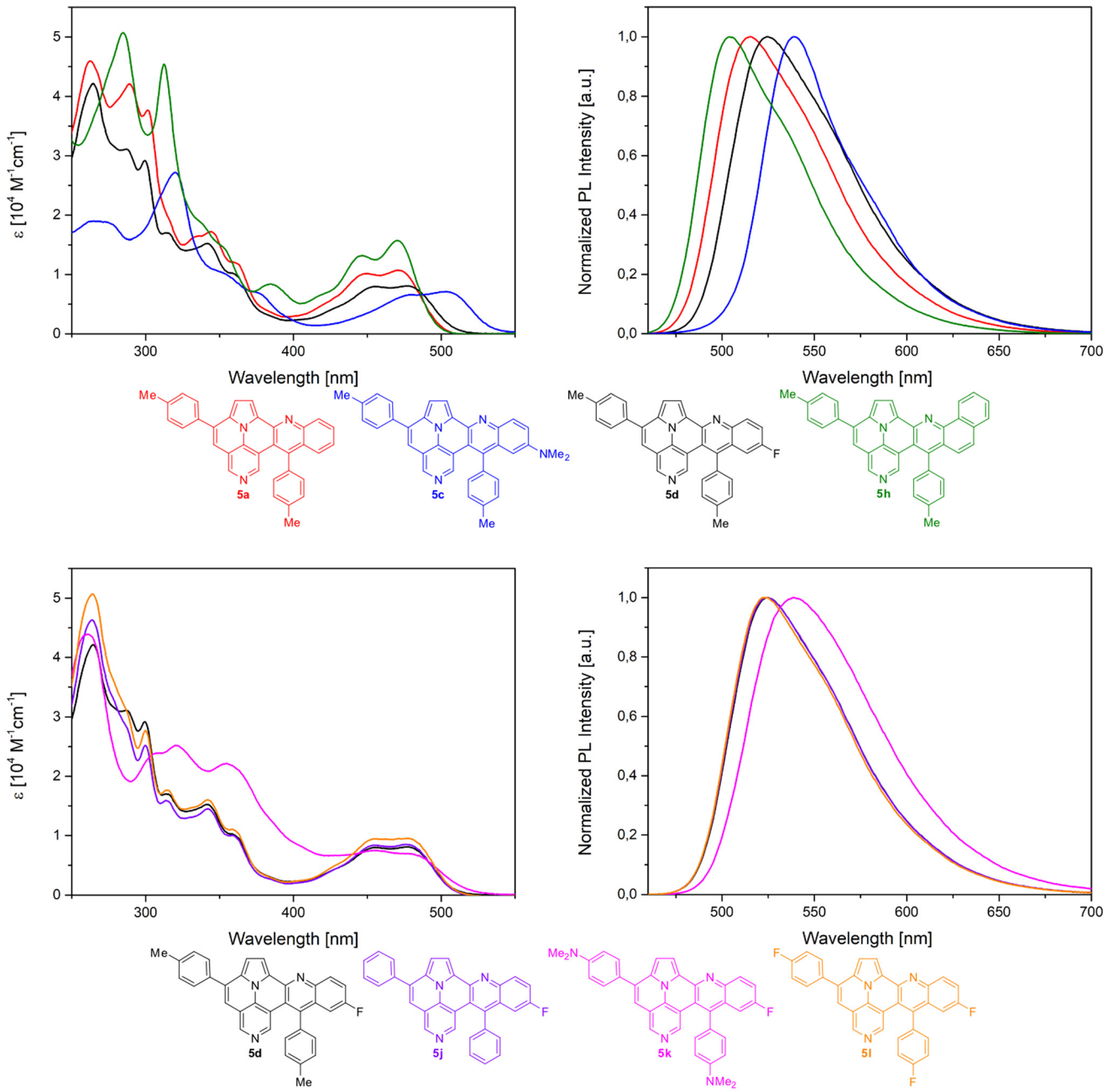

Fig. 4 UV/Vis- (top/bottom, left) and PL-spectra (top/bottom, right, λ_{ex} = 450 nm) of shown compounds in DCM (c = 10^{-5} M) at 20 °C.

Table 4 Spectroscopic data of **5a**, **5c**, **5d**, **5h**, **5j**, **5k** and **5l** in DCM (c = 10^{-5} M) at 20 °C

	5a	**5c**	**5d**	**5h**	**5j**	**5k**	**5l**
$\lambda_{1,abs}$ [nm]	471	503	477	470	477	482	480
ε_{λ_1} [10^4 L mol^{-1} cm^{-1}]	1.1	0.7	0.8	1.6	0.8	0.7	0.9
$\lambda_{2,abs}$ [nm]	448	480	454	447	477	455	455
ε_{λ_2} [10^4 L mol^{-1} cm^{-1}]	1.0	0.7	0.8	1.3	0.8	0.7	0.9
$\lambda_{1,em}$ [nm]	515	539	525	505	524	539	524
E_g^{opt} [eV] [a]	2.56	2.42	2.53	2.59	2.53	2.50	2.53
Φ [b]	0.26	0.19	0.27	0.35	0.25	0.20	0.28

[a] Determined from the intersection of the normalized absorption and emission spectra. [b] Fluorescence standard: quinine hemisulfate monohydrate in 0.05 M H_2SO_4 (Φ = 0.52).[22]

5c between cyclohexane and ethanol, indicating that the NMe_2-group of **5c** has only negligible effect on the ICT character of the core structure. In contrast, a stronger shift of 59 nm can be observed for **5k**. For all compounds, a decrease of the emission in more polar solvents is observed and accompanied by a reduction of their quantum yields (ESI, Table 5†). However, **5k** again behaves quite differently from **5a** and **5c** and shows only very weak fluorescence in acetonitrile and ethanol with quantum yields ≤ 1%, what might be explained by the occurrence of a twisted intramolecular charge transfer (TICT). This effect appears in polar acetonitrile and ethanol, suggesting that the polarity of the solvent

Table 5 Comparison of optical properties with related molecular structures

	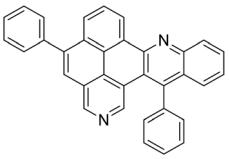 Quinolino-azapyrene[19]	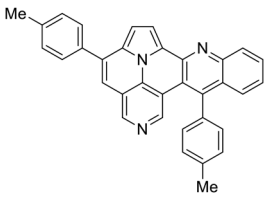 5a	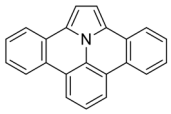 Dibenzo-ullazine[9]	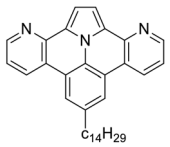 Dipyrido-ullazine[15]
$\lambda_{1,abs}$ [nm]	415	471	~420[a]	~425[a]
ε_{λ_1} [10^4 L mol^{-1} cm^{-1}]	1.0	1.1	—	—
$\lambda_{1,em}$ [nm]	430	515	444	~450[a]
Φ	0.47	0.26	0.35	—

[a] Estimated from the graphs.

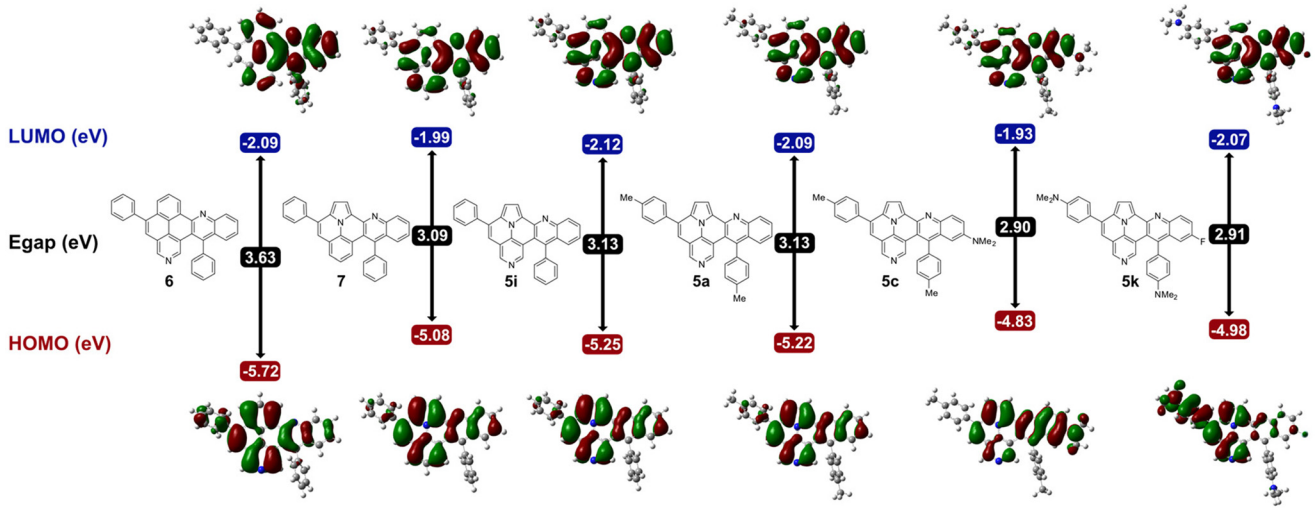

Fig. 5 Frontier orbitals of selected compounds and energy levels calculated at the B3LYP/6-31G(d,p) level of theory within IEFPCM in DCM.

may sufficient to stabilize a TICT. This twisted structure may explain the quenching of the fluorescence through the radiation-free TICT-relaxation.[26]

Further investigations of the ICT-character were performed by calculations of the dipole moments of the ground (S_0) and excited state (S_1) of **5a**, **5c** and **5k**. These calculations confirm the results of the studies related to solvatochromism. Compound **5k** (μ_{S_0} = 4.4193; μ_{S_1} = 26.2043) indicates the strongest increase in the dipole moment, followed by **5a** (μ_{S_0} = 1.0280; μ_{S_1} = 10.6564) and **5c** (μ_{S_0} = 4.1596; μ_{S_1} = 6.0825).

In addition, we performed protonation studies with trifluoromethanesulfonic acid (TFA) in DCM for compound **5a**. As shown in Fig. 7, protonation of **5a** results in a bathochromic shift in the absorption and emission spectra. The first absorption maximum shifts from 471 nm for the free base **5a** to 534 nm for protonated species and an isosbestic point at a wavelength of 482 nm can be detected. The PL-spectra show similar results: the emission maximum shifts from 515 nm to 586 nm, with the first emission maximum decreasing and the second increasing simultaneously. In addition, protonation results, beside the bathochromic shift, also in a decrease of fluorescence. However, changes and shapes of the absorption and PL spectra during the protonation experiments prohibit conclusion whether only one or both pyridinic nitrogen are protonated.

Finally, we performed nuclear-independent chemical shift (NICS) calculations for the quinolino-azaullazine core structure (**5′**) to gain insight into the aromatic behavior of the compound. Therefore, NICS(1.25)$_{zz}$ values were calculated for each ring to investigate the local aromaticity.[27] Furthermore, ring currents were calculated using the BC-Wizard program developed by Gershoni-Poranne *et al.*[28] The calculations were performed in comparison to quinolino-azapyrene **6′** and quinolino-ullazine **7′** (Fig. 8).[19] All three compounds display a global diatropic ring current, as well as negative NICS$_{zz}$ values in all rings. In addition, all studied compounds exhibit two semiglobal ring currents, one in the quinoline moiety, the other in the benzo-isoquinoline or pyrrolo-quinoline moiety. However, the

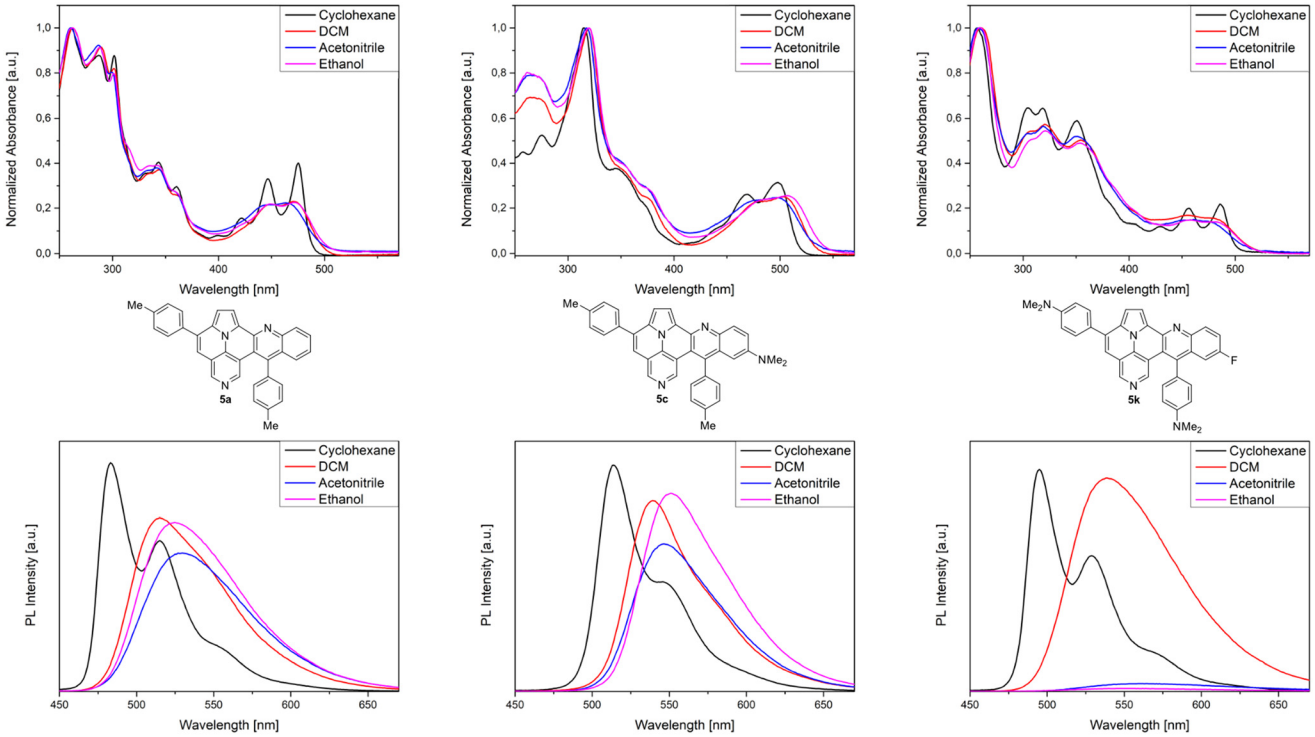

Fig. 6 Top: UV/Vis-spectra of **5a** (left), **5c** (middle), **5k** (right); Bottom: PL-spectra **5a** (left), **5c** (middle), **5k** (right), *t*, λ_{ex} = 340 nm; spectra measured with toluene, dichloromethane, acetonitrile and ethanol ($c = 10^{-5}$ M at 20 °C).

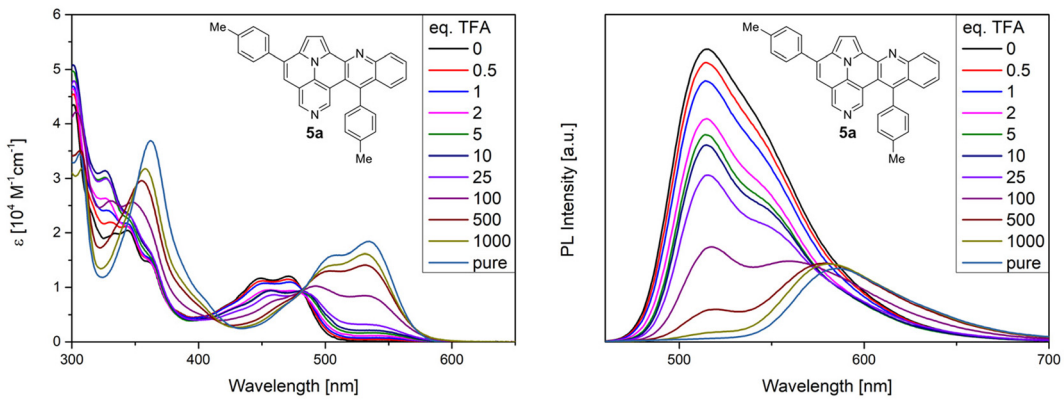

Fig. 7 Absorption and PL spectra of **5a** in dependence of the TFA concentration.

connecting ring of both moieties is not involved in any semi-global ring current, thus the molecules consist of two aromatic subunits connected by a ring with non-aromaticity in case of **5′** and **7′**, and low aromaticity for **6′**, which is confirmed by the $NICS_{zz}$ values. In the two ullazine structures, this ring shows even lower aromaticity than in the aza-pyrene structure. In addition, the ring current maps show that there is a difference mainly in the benzoisoquinoline or pyrroloquinoline moiety, which is due to the different molecular structure. Thus, **6′** shows a stronger semiglobal current, whereas **5′** and **7′** exhibit a stronger local ring current focused on the pyrrole unit. Comparing the structures of ullazine **7′** and azaullazine **5′**, only negligible differences are noticed, as both have almost the same ring currents and similar $NICS_{zz}$ values. Hence, the impact on aromaticity by the presence of an additional nitrogen of **7′** as compared to **5′** is very small. However, a pronounced influence is observed by incorporation of an ullazine as compared to a related azapyrene sub-structure.

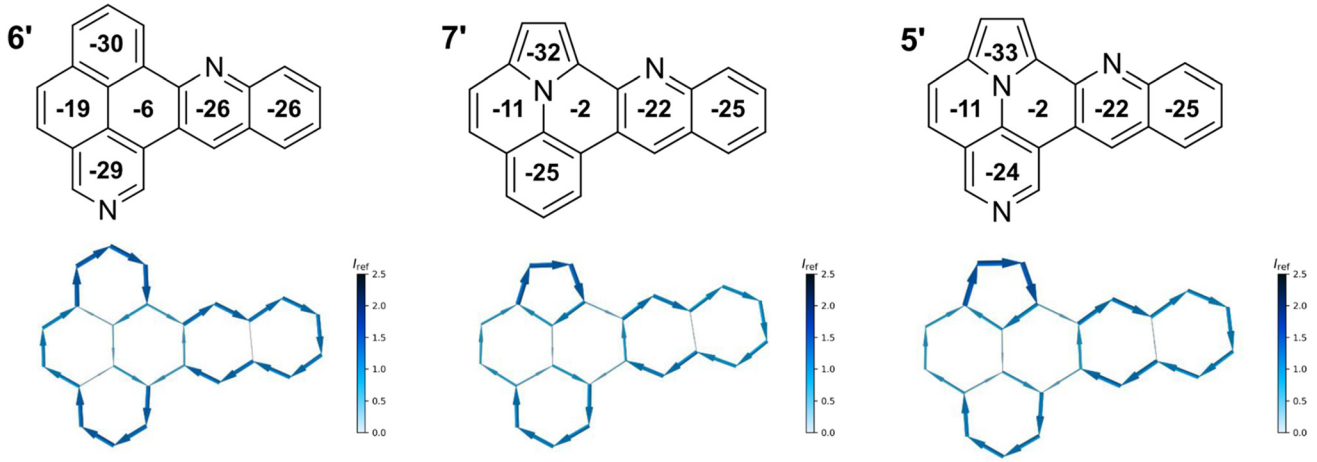

Fig. 8 NICS calculations for benzo[*j*]naphtho[2,1,8-*def*][2,7]phenanthroline (**6'**); indolizino[6,5,4,3-*ija*]quinolino[2,3-*c*]quinoline (**7'**); indolizino[6,5,4,3-*ija*]quinolino[2,3-*c*][1,6]naphthyridine (**5'**). Top: Scheme of molecule with respective NICS(1.25)$_{zz}$ values in the center of each ring. Bottom: NICS2BC graphs (current was calculated form NICS(1.25)$_{zz}$ strength relative to I_{ref} (ring current of benzene, 11.5 nA T^{-1})).[28]

Conclusion

Hitherto unknown quinolino-azaullazines were prepared by combination of Pd catalyzed cross-coupling with Povarov reactions. The synthetic strategy provides a convenient access to various functionalized molecules, which allowed for a fine-tuning of the optical properties. Especially the variation of the aniline component in the Povarov reaction has an important impact on the optoelectronic properties of the products. All investigated compounds exhibit strong absorption in visible light as well as greenish fluorescence with quantum yields between 19% and 35%. Noteworthy is the introduction of strongly donating NMe_2-substituents, which cause extensive alternation of the optical properties not only attached to the core structure, but also on the phenyl substituents. Solvatochromism studies revealed that an ICT character is already present in the core structure, independently from the substitution pattern. However, the presence of a NMe_2-group at the phenyl groups even improved the ICT properties, which suggests the presence of TICT. Further modification of the optical properties was achieved by protonation, which causes a red shift of both absorption and emission. Cyclic voltammetry investigation revealed a more facile oxidation as compared to quinolinoazapyrenes, due to the strong donor capacity of the azaullazine core structure. These observations were confirmed by DFT calculations. NICS calculations disclosed that the novel aza-PAHs prepared have a weak global ring current and can be best described by the presence of two independent aromatic systems consisting of a pyrroloquinoline and a quinoline unit connected by a non-aromatic ring. Further studies will focus on the synthesis of related heteroatom doped PAHs by means of the Povarov reaction.

Experimental section

General information

The nuclear magnetic resonance spectra (^{1}H/^{13}C/^{19}F NMR) were recorded on a Bruker AVANCE 300 III, 250 II, or 500. The analyzed chemical shifts δ are referenced to residual solvents signals of the deuterated solvents $CDCl_3$ (δ = 7.26 ppm/77.0 ppm). Multiplicities due to spin–spin correlation are reported as follows, s = singlet, d = doublet, dd = double doublet, ddd = doublets of doublets, m = multiplet, and further described through their coupling constants *J*. Infrared spectra (IR) were measured as attenuated total reflection (ATR) experiments with a Nicolet 380 FT-IR spectrometer. The signals have been characterized through their wave numbers $\tilde{\nu}$ and their corresponding absorption as very strong (vs), strong (s), medium (m) or weak (w). UV/Vis spectra were recorded on a Cary 60 UV-vis spectrophotometer and emission spectra with an Agilent Cary Eclipse fluorescence spectrophotometer. Cyclic voltammograms were measured at room temperature in DCM or THF ($c = 10^{-3}$ M) with 0.1 M *n*-Bu_4NPF_6 as a supporting electrolyte, glassy carbon working electrode, ANE2 ($Ag/AgNO_3$ 0.01 M in CH_3CN) as reference electrode and Pt counter-electrode (0.5 mm diameter platinum wire) with ferrocene ($c = 10^{-3}$ M, in CH_3CN) as an external standard at a scan rate of 100 mV s^{-1} or 200 mV s^{-1}. The potentiostat used was a PalmSense EmStat 3 blue or a Parstat 4000 from Ametek. The working electrode is a 3 mm diameter (length 80, 6.35 mm outer diameter) glassy carbon disk electrode in a KeI-F coating that was polished on a polishing pad in aqueous alumina slurry (0.03 μm alumina powder). The solvents were deoxygenated by purging with argon. The potential is given *vs.* Fc/Fc^+. The direction of scan is reductive with a starting potential of 1.5 V and a switching potential of −1.5 V for DCM and for THF a starting potential of 0 V and a switching potential of −3.2 V. CVs are plotted using the IUPAC. Basic and high-resolution mass spectra (MS/HRMS) were measured on instruments which are paired with a preceding gas chromatograph (GC) or liquid chromatograph (LC). The samples have been ionized through electron impact ionization (EI) on an Agilent 6890/5973 or Agilent 7890/5977 GC-MS equipped with a HP-5 capillary column using helium carrier gas or by applying electron spray ionization (ESI) on an

Agilent 1200/6210 Time-of-Flight (TOF) LC-MS. Melting points (mp) were determined by a Micro-Hot-Stage GalenTM III Cambridge Instruments and are not corrected. X-ray single-crystal structure analysis was performed on a Bruker Apex Kappa-II CCD diffractometer.

Analytical data

3,5-Dibromo-4-(1*H*-pyrrol-1-yl)pyridine (1). Starting from 4-aminopyridine, **1** could be synthesized according to the literature-known procedure in a yield of 77% (5.14 g) yield.[5] The NMR data agree with the published NMR data. **^{1}H NMR** (250 MHz, $CDCl_3$) δ = 8.77 (s, 2H), 6.74–6.72 (m, 2H), 6.47–6.38 (m, 2H). **^{13}C NMR** (63 MHz, $CDCl_3$) δ = 151.7 (CH), 146.5, 121.0 (C), 120.9, 110.3 (CH).

1-(3,5-Dibromopyridin-4-yl)-1*H*-pyrrole-2-carbaldehyde (2a). 3,5-Dibromo-4-(1*H*-pyrrol-1-yl)pyridine (**1**, 1.00 g, 3.31 mmol) was suspended in 5 ml DMF in a Schlenk flask under an argon atmosphere. 2 eq. $POCl_3$ (6.62 mmol, 0.63 ml) were added dropwise at 0 °C. The solution was stirred at 100 °C for 3 h, cooled to room temperature, neutralized with $NaHCO_3$ and extracted with DCM. The combined organic phases were dried with Na_2SO_4, the solvent was removed *in vacuo* and the residue was purified by column chromatography to give **2a** as a colourless solid (0.364 g, 33%). **Mp** 129 °C. R_f 0.22 (heptane/ethyl acetate 3 : 1). **^{1}H NMR** (300 MHz, $CDCl_3$) δ = 9.49 (d, ^4J = 1.0 Hz, 1H), 8.69 (s, 2H), 7.09 (dd, ^3J = 3.9 Hz, ^4J = 1.6 Hz, 1H), 6.81 (ddd, ^3J = 2.7 Hz, ^4J = 1.6 Hz, ^4J = 1.0 Hz, 1H), 6.49 (dd, ^3J = 4.0 Hz, ^3J = 2.7 Hz, 1H). **^{13}C NMR** (75 MHz, $CDCl_3$) δ = 178.2 (CHO), 151.3 (CH), 145.9, 131.7 (C), 129.1, 123.6 (CH), 121.2 (C), 112.3 (CH). **IR** (ATR, cm^{-1}): $\tilde{\nu}$ = 1661 (s), 1484 (m), 1399 (m), 1356 (s), 1199 (m), 1037 (m), 999 (m), 886 (m), 779 (s), 750 (s), 715 (m), 610 (m), 577 (s). **MS** (EI, 70 eV): *m*/*z* (%) = 330 ([M]$^+$, 1), 252 (11), 251 (98), 250 (15), 249 (100), 170 (21), 142 (8), 130 (5), 115 (9), 114 (7). **HRMS** (EI): calculated for $C_{10}H_6{}^{79}Br_2N_2O$ ([M]$^+$) 327.88414, found 327.88451; calculated for $C_{10}H_6{}^{79}Br^{81}BrN_2O$ ([M]$^+$) 329.88209, found 329.88255; calculated for $C_{10}H_6{}^{81}Br_2N_2O$ ([M]$^+$) 331.88005, found 331.88075.

1-(3,5-Dibromopyridin-4-yl)-1*H*-pyrrole-3-carbaldehyde (2b). Using the reaction conditions as for **2a**, the main product **2b** was obtained after column chromatography (3 : 1 heptane : ethyl acetate) as a colourless solid (0.673 g, 62%). **Mp** 100–110 °C. R_f 0.14 (heptane/ethyl acetate 3 : 1). **^{1}H NMR** (300 MHz, $CDCl_3$) δ = 9.89 (dd, ^4J = 0.4 Hz, 1H), 8.81 (s, 2H), 7.34 (dd, ^4J = 2.1 Hz, ^4J = 1.6 Hz, 1H), 6.87 (ddd, ^3J = 3.1 Hz, ^4J = 1.6 Hz, ^4J = 0.4 Hz, 1H), 6.74 (ddd, ^3J = 3.0 Hz, ^4J = 2.1 Hz, ^4J = 0.7 Hz, 1H). **^{13}C NMR** (75 MHz, $CDCl_3$) δ = 185.2 (CHO), 152.0 (CH), 145.1 (C), 128.9 (CH), 128.3 (C), 123.6 (CH), 120.5 (C), 109.3 (CH). **IR** (ATR, cm^{-1}): $\tilde{\nu}$ = 1675 (s), 1508 (s), 1467 (s), 1294 (m), 1257 (m), 1210 (m), 1152 (m), 1084 (m), 1041 (s), 816 (m), 732 (s), 618 (m), 591 (m). **MS** (EI, 70 eV): *m*/*z* (%) = 332 (34), 331 (54), 330 ([M]$^+$, 69), 329 (100), 328 (36), 327 (50), 142 (7), 141 (10), 130 (6), 128 (6), 114 (7). **HRMS** (ESI-TOF): calculated for $C_{10}H_7Br_2N_2O$ ([M + H]$^+$) 328.8925, found 328.8931.

General procedure A for the synthesis of 1-(3,5-bis(arylethynyl)pyridin-4-yl)-1*H*-pyrrole-2-carbaldehyde (3a–e). In a pressure tube, 200 mg of 1-(3,5-dibromopyridin-4-yl)-1*H*-pyrrole-2-carbaldehyde (**2a**), 0.05 eq. $PdCl_2(PPh_3)_2$, 0.05 eq. CuI, 0.1 eq. cataCXium A were dissolved in 0.5 ml HN^iPr_2 and 3 mL of 1,4-dioxane under argon counter current. Then, 3 eq. of the respective alkyne was added to the solution with stirring. The pressure tube was sealed with a Teflon cap and the solution was stirred for 24 h at 90 °C. The reaction solution was cooled to room temperature, quenched with distilled water and extracted three times with DCM. The combined organic phases were dried over Na_2SO_4, the solvent was distilled off *in vacuo*, and the residue was purified by column chromatography (Hep/EtOAc) to give the desired products (**3a–e**).

1-(3,5-Bis(phenylethynyl)pyridin-4-yl)-1*H*-pyrrole-2-carbaldehyde (3a). According to general procedure A, the title compound **3a** was obtained as a yellow-orange solid in 80% yield (181 mg). **Mp** 118–122 °C. R_f 0.14 (heptane/ethyl acetate 5 : 1). **^{1}H NMR** (300 MHz, $CDCl_3$) δ = 9.60 (d, ^4J = 0.8 Hz, 1H), 8.80 (s, 2H), 7.34–7.28 (m, 10H), 7.24 (dd, ^3J = 3.9 Hz, ^4J = 1.6 Hz, 1H), 7.19 (ddd, ^3J = 2.6 Hz, ^4J = 1.6 Hz, ^4J = 0.9 Hz, 1H), 6.58 (dd, ^3J = 3.9 Hz, ^3J = 2.7 Hz, 1H). **^{13}C NMR** (75 MHz, $CDCl_3$) δ = 178.2 (CHO), 151.8 (CH), 148.2, 132.9 (C), 131.6, 130.5, 129.2, 128.3, 122.4 (CH), 121.7, 118.8 (C), 111.3 (CH), 97.2, 81.6 (C≡C). **IR** (ATR, cm^{-1}): $\tilde{\nu}$ = 1659 (s), 1480 (m), 1403 (m), 1354 (m), 1036 (m), 890 (m), 781 (s), 748 (s), 686 (s), 573 (m), 548 (m). **MS** (EI, 70 eV): *m*/*z* (%) = 372 ([M]$^+$, 19), 345 (25), 344 (100), 343 (47), 342 (40), 341 (11), 340 (14), 316 (8), 315 (9), 266 (10), 171 (5), 158 (4). **HRMS** (ESI-TOF): calculated for $C_{26}H_{17}N_2O$ ([M + H]$^+$) 373.1341, found 373.1349.

1-(3,5-Bis(*p*-tolylethynyl)pyridin-4-yl)-1*H*-pyrrole-2-carbaldehyde (3b). According to general procedure A, the title compound **3b** was obtained as a yellow-orange solid in 76% yield (193 mg). **Mp** 123–125 °C. R_f 0.21 (heptane/ethyl acetate 5 : 1), **^{1}H NMR** (500 MHz, $CDCl_3$) δ = 9.59 (d, ^4J = 0.8 Hz, 1H), 8.77 (s, 2H), 7.23 (dd, ^3J = 4.0 Hz, ^4J = 1.6 Hz, 1H), 7.20 (d, ^3J = 8.2 Hz, 4H), 7.18–7.17 (m, 1H), 7.11 (d, ^3J = 7.9 Hz, 4H), 6.56 (dd, ^3J = 4.0 Hz, ^3J = 2.7 Hz, 1H), 2.34 (s, 6H). **^{13}C NMR** (126 MHz, $CDCl_3$) δ = 178.2 (CHO), 151.5 (CH), 147.9, 139.5 (C), 132.9, 131.5, 130.4, 129.1 (CH), 119.0, 118.7 (C), 111.2 (CH), 97.6, 81.1 (C≡C), 21.5 (CH_3). **IR** (ATR, cm^{-1}): $\tilde{\nu}$ = 1657 (s), 1508 (m), 1484 (m), 1407 (s), 1356 (m), 1030 (m), 886 (m), 814 (s), 785 (s), 754 (s), 743 (s), 577 (s), 528 (s). **MS** (EI, 70 eV): *m*/*z* (%) = 400 ([M]$^+$, 14), 373 (29), 372 (100), 371 (23), 370 (11), 369 (9), 357 (10), 356 (17), 178 (9), 177 (9). **HRMS** (ESI-TOF): calculated for $C_{28}H_{21}N_2O$ ([M + H]$^+$) 401.1654, found 401.1643.

1-(3,5-Bis((4-fluorphenyl)ethynyl)pyridin-4-yl)-1*H*-pyrrole-2-carbaldehyde (3c). According to general procedure A, the title compound **3c** was obtained as yellow solid in 87% yield (216 mg). **Mp** 129–132 °C. R_f 0.19 (heptane/ethyl acetate 5 : 1). **^{1}H NMR** (300 MHz, $CDCl_3$) δ = 9.54 (d, ^4J = 0.8 Hz, 1H), 8.73 (s, 2H), 7.27–7.17 (m, 5H), 7.12 (ddd, ^3J = 2.6 Hz, ^4J = 1.6 Hz, ^4J = 0.9 Hz, 1H), 6.98–6.91 (m, 4H), 6.53 (dd, ^3J = 3.9 Hz, ^3J = 2.7 Hz, 1H). **^{13}C NMR** (75 MHz, $CDCl_3$) δ = 178.2 (CHO), 163.0 (d, ^1J = 251.4 Hz, C), 151.7 (CH), 148.1 (C), 133.6 (d, ^3J = 8.6 Hz, CH), 132.9 (C), 130.4, 122.4 (CH), 118.7 (C), 117.8 (d, ^4J = 3.5 Hz, C), 115.8 (d, ^2J = 22.2 Hz, C), 111.3 (C), 96.2 (C≡C), 81.4 (d, ^5J = 1.5 Hz, C≡C). **^{19}F NMR** (282 MHz, $CDCl_3$): δ = −108.8.

IR (ATR, cm^{-1}): $\tilde{\nu}$ = 1667 (s), 1504 (s), 1407 (s), 1226 (s), 1154 (m), 1092 (m), 832 (s), 783 (m), 742 (s), 575 (m), 528 (s), 492 (s). **MS** (EI, 70 eV): *m*/*z* (%) = 408 ([M]$^+$, 17), 381 (26), 380 (100), 379 (43), 378 (36), 377 (7), 376 (9), 352 (6), 351 (7), 313 (4), 284 (9), 189 (4). **HRMS** (ESI-TOF): calculated for $C_{26}H_{15}F_2N_2O$ ([M + H]$^+$) 409.1152, found 409.1149.

1-(3,5-Bis((4-(trifluoromethyl)phenyl)ethynyl)pyridin-4-yl)-1*H*-pyrrole-2-carbaldehyde (3d). According to general procedure A, the title compound **3d** was obtained as a yellow solid in 74% yield (228 mg). **Mp** 135–142 °C. R_f 0.10 (heptane/ethyl acetate 10 : 1). **^{1}H NMR** (300 MHz, $CDCl_3$) δ = 9.52 (d, ^4J = 0.9 Hz, 1H), 8.75 (s, 2H), 7.48 (d, ^3J = 8.1 Hz, 4H), 7.30 (d, ^3J = 7.9 Hz, 4H), 7.17 (dd, ^3J = 3.9 Hz, ^4J = 1.6 Hz, 1H), 7.10 (ddd, ^3J = 2.6 Hz, ^4J = 1.6 Hz, ^4J = 0.9 Hz, 1H), 6.52 (dd, ^3J = 3.9 Hz, ^3J = 2.7 Hz, 1H). **^{13}C NMR** (75 MHz, $CDCl_3$) δ = 178.2 (CHO), 152.4 (CH), 148.9, 132.9 (C), 131.9 (CH), 130.9 (q, ^2J = 32.8 Hz, C), 130.5 (CH), 125.4 (C), 125.3 (q, ^3J = 3.8 Hz, CH), 123.6 (q, ^1J = 272.2 Hz, C), 123.0 (CH), 118.3 (C), 111.5 (CH), 95.6, 83.6 (C≡C). **^{19}F NMR** (282 MHz, $CDCl_3$): δ = −63.0. **IR** (ATR, cm^{-1}): $\tilde{\nu}$ = 1663 (s), 1613 (m), 1484 (m), 1405 (m), 1319 (s), 1164 (s), 1102 (s), 1063 (s), 1016 (s), 839 (s), 781 (m), 740 (s), 575 (m). **MS** (EI, 70 eV): *m*/*z* (%) = 508 ([M]$^+$, 23), 481 (27), 480 (100), 479 (30), 478 (13), 461 (7), 411 (9), 410 (19), 363 (5), 334 (6), 195 (7). **HRMS** (ESI-TOF): calculated for $C_{28}H_{15}F_6N_2O$ ([M + H]$^+$) 509.1089, found 509.1096.

1-(3,5-Bis((4-(dimethylamino)phenyl)ethynyl)pyridin-4-yl)-1*H*-pyrrole-2-carbaldehyde (3e). According to general procedure A, the title compound **3e** was obtained as a yellow-brown solid in 45% yield (125 mg). **Mp** 175–183 °C. R_f 0.13 (heptane/ethyl acetate 3 : 1). **^{1}H NMR** (300 MHz, $CDCl_3$) δ = 9.57 (d, ^4J = 0.7 Hz, 1H), 8.68 (s, 2H), 7.23 (dd, ^3J = 3.9 Hz, ^4J = 1.6 Hz, 1H), 7.20–7.14 (m, 5H), 6.59–6.53 (m, 5H), 2.95 (s, 12H). **^{13}C NMR** (75 MHz, $CDCl_3$) δ = 178.2 (CHO), 150.4 (C), 150.3 (CH), 146.4, 132.8 (C), 132.8, 132.5, 130.4 (CH), 119.5 (C), 111.5, 110.8 (CH), 108.2 (C), 99.1, 80.2 (C≡C), 39.9 (CH_3). **IR** (ATR, cm^{-1}): $\tilde{\nu}$ = 1667 (s), 1603 (s), 1564 (s), 1519 (s), 1480 (s), 1360 (s), 1232 (m), 1168 (s), 806 (s), 783 (s), 740 (s), 577 (m), 523 (m). **MS** (EI, 70 eV): *m*/*z* (%) = 458 ([M]$^+$, 100), 457 (23), 431 (15), 430 (57), 429 (22), 414 (22), 229 (14), 215 (12), 214 (25), 206 (12), 192 (11). **HRMS** (ESI-TOF): calculated for $C_{30}H_{27}N_4O$ ([M + H]$^+$) 459.2185, found 459.2189.

14-(*p*-Tolyl)-4-(*p*-tolylethynyl)pyrrolo[1,2-*a*]quinolino[2,3-*c*][1,6]naphthyridine (4). **3a** (150 mg) is dissolved in toluene (3.0 ml) together with aniline (1.2 eq.), then $FeCl_3$ (0.01 eq.) was added. The solution was stirred at 100 °C for 2 h. The reaction solution was cooled to room temperature, quenched with distilled water and extracted three times with DCM. The combined organic phases were dried over Na_2SO_4, the solvent was distilled off *in vacuo*, and the residue was purified by column chromatography (Hep/EtOAc) to give the desired product **4** in 86% (153 mg). **Mp** > 375 °C. R_f 0.26 (heptane/ethyl acetate 5 : 1). **^{1}H NMR** (300 MHz, $CDCl_3$) δ = 9.37 (dd, ^3J = 3.1 Hz, ^4J = 1.5 Hz, 1H), 8.63 (s, 1H), 8.46 (s, 1H), 8.14 (d, ^3J = 8.4 Hz, 1H), 7.71 (ddd, ^3J = 8.4 Hz, ^3J = 6.7 Hz, ^4J = 1.4 Hz, 1H), 7.66 (dd, ^3J = 3.8 Hz, ^4J = 1.5 Hz, 1H), 7.57 (dd, ^3J = 8.6 Hz, ^4J = 1.5 Hz, 1H), 7.54–7.50 (m, 2H), 7.43 (d, ^3J = 7.7 Hz, 2H), 7.37 (ddd, ^3J = 8.4 Hz, ^3J = 6.7 Hz, ^4J = 1.3 Hz, 1H), 7.32–7.19 (m, 4H), 6.80 (dd, ^3J = 3.8 Hz, ^3J = 3.1 Hz, 1H), 2.53 (s, 3H), 2.41 (s, 3H). **^{13}C NMR** (75 MHz, $CDCl_3$) δ = 153.7, 148.2, 145.6, 144.8, 139.6, 138.8, 135.2 (C), 131.3 (C), 131.3, 130.7, 130.2, 129.4, 129.2, 128.8 (CH), 127.1 (C), 126.9, 125.7, 120.3 (CH), 119.3, 115.9 (C), 113.5, 109.5 (CH), 97.9, 85.6 (C≡C), 21.6, 21.5 (CH_3). **IR** (ATR, cm^{-1}): $\tilde{\nu}$ = 1737 (s), 1597 (s), 1504 (s), 1451 (s), 1356 (s), 1205 (s), 1028 (s), 960 (m), 812 (s), 762 (s), 690 (s), 604 (m). **MS** (EI, 70 eV): *m*/*z* (%) = 473 ([M]$^+$, 100), 472 (87), 471 (21), 470 (9), 459 (7), 458 (24), 457 (22), 456 (11), 229 (10), 228 (12). **HRMS** (ESI-TOF): calculated for $C_{34}H_{24}N_3$ ([M + H]$^+$) 474.1970, found 474.1978.

General procedure B for the synthesis of 5,13-di-arylindolizino[6,5,4,3-*ija*]quinolino[2,3-*c*][1,6]naphthyridines (5a–l). 150 mg of **3a–e** together with 1.2 eq. of corresponding aniline and 0.1 eq. $FeCl_3$ (1 eq. for **5c**) were suspended in 3 ml toluene and stirred at 100 °C for 2 h (4 h for **5i**). Subsequently, the solution was diluted with water and extracted with DCM. The combined organic phases were dried over Na_2SO_4, the solvent was distilled off *in vacuo*. The crude product was dissolved in xylene and 20 eq. *p*-TsOH·H_2O were added. The solution was stirred at 120 °C for 6 h (20 h for **5i** and **5k**). The reaction was quenched with $NaHCO_3$-solution, extracted with DCM and dried over Na_2SO_4. The solvent was distilled off *in vacuo* and the residue was purified by column chromatography (Hep/EtOAc) to give the desired products (**5a–l**).

mmol-scale procedure for the synthesis 5,13-di-*p*-tolylindolizino[6,5,4,3-*ija*]quinolino[2,3-*c*][1,6]naphthyridine (5a). 480 mg (1.2 mmol) of **3a** together with 1.2 eq. aniline (131 µl) and 0.1 eq. $FeCl_3$ (19 mg) were suspended in 10 ml toluene and stirred at 100 °C for 2 h. Subsequently, the solution was diluted with water and extracted with DCM. The combined organic phases were dried over Na_2SO_4, the solvent was distilled off *in vacuo*. The crude product was dissolved in xylene and 20 eq. *p*-TsOH·H_2O (4.55 g) were added. The solution was stirred at 120 °C for 6 h. The reaction was quenched with $NaHCO_3$-solution, extracted with DCM and dried over Na_2SO_4. The solvent was distilled off *in vacuo* and the residue was purified by column chromatography (Hep/EtOAc) to give desired products **5a** in 47% (224 mg) yield.

5,13-Di-*p*-tolylindolizino[6,5,4,3-*ija*]quinolino[2,3-*c*][1,6]naphthyridine (5a). According to general procedure B, the title compound **5a** was obtained as a orange solid in 47% yield (83 mg). **Mp** 242–247 °C; R_f 0.29 (heptane/ethyl acetate 2 : 1). **^{1}H NMR** (300 MHz, $CDCl_3$) δ = 8.74 (s, 1H), 8.13 (ddd, ^3J = 8.5 Hz, ^4J = 1.3 Hz, ^5J = 0.6 Hz, 1H), 8.03 (s, 1H), 7.95 (d, ^3J = 4.2 Hz, 1H), 7.73–7.64 (m, 3H), 7.52–7.46 (m, 3H), 7.39–7.27 (m, 5H), 7.14 (s, 1H), 7.09 (d, ^3J = 4.2 Hz, 1H), 2.57 (s, 3H), 2.47 (s, 3H). **^{13}C NMR** (75 MHz, $CDCl_3$) δ = 148.1, 146.4 (C), 145.0, 144.8 (CH), 144.8, 138.9, 138.7, 135.3, 134.8, 134.3, 134.0 (C), 130.9, 130.3, 129.5 (CH), 129.2 (C), 128.6, 128.0 (CH), 127.3 (C), 127.0 (CH), 126.2 (C), 125.7 (CH), 119.8, 117.5, 117.2 (C), 115.3, 111.2, 107.1 (CH), 21.6, 21.3 (CH_3). **IR** (ATR, cm^{-1}): $\tilde{\nu}$ = 2920 (m), 1539 (m), 1502 (m), 1445 (m), 1358 (m), 1179 (m), 1109 (m), 1041 (m), 892 (m), 816 (s), 758 (s), 734 (s), 610 (m), 490 (s). **MS** (EI, 70 eV): *m*/*z* (%) = 473 ([M]$^+$, 100), 472 (69), 471 (72), 470

(17), 457 (17), 456 (18), 236 (46), 235 (16), 228 (37), 227 (24), 226 (12), 220 (12). **HRMS** (ESI-TOF): calculated for $C_{34}H_{24}N_3$ ($[M + H]^+$) 474.1970, found 474.1977.

11-Methyl-5,13-di-*p*-tolylindolizino[6,5,4,3-*ija*]quinolino[2,3-*c*][1,6]naphthyridine (5b). According to general procedure B, the title compound **5b** was obtained as a yellow solid in 44% yield (82 mg). **Mp** 271–275 °C; R_f 0.34 (heptane/ethyl acetate 2 : 1). **^{1}H NMR** (300 MHz, $CDCl_3$) δ = 8.74 (s, 1H), 8.05 (d, ^3J = 8.6 Hz, 1H), 7.99 (s, 1H), 7.95 (d, ^3J = 4.2 Hz, 1H), 7.71–7.66 (m, 2H), 7.54 (dd, ^3J = 8.6 Hz, ^4J = 2.0 Hz, 1H), 7.52–7.47 (m, 2H), 7.37–7.32 (m, 2H), 7.32–7.27 (m, 2H), 7.24–7.22 (m, 1H), 7.15 (s, 1H), 7.10 (d, ^3J = 4.1 Hz, 1H), 2.58 (s, 3H), 2.47 (s, 3H), 2.41 (s, 3H). **^{13}C NMR** (75 MHz, $CDCl_3$) δ = 146.8, 145.7 (C), 145.0, 144.7 (CH), 144.1, 138.8, 138.7, 135.7, 135.5, 134.9, 134.3, 134.0 (C), 132.7, 130.9, 129.6 (CH), 129.0 (C), 128.7, 128.4, 128.0 (CH), 127.3, 126.3 (C), 125.6 (CH), 119.8, 117.7, 117.2 (C), 115.2, 110.8, 107.0 (CH), 21.9, 21.6, 21.4 (CH_3). **IR** (ATR, cm^{-1}): $\tilde{\nu}$ = 1502 (m), 1354 (m), 1183 (m), 1109 (m), 1036 (m), 884 (m), 814 (s), 802 (s), 781 (s), 711 (m), 602 (m), 488 (s). **MS** (EI, 70 eV): *m*/*z* (%) = 487 ($[M]^+$, 100), 486 (55), 485 (11), 472 (18), 471 (24), 470 (11), 457 (6), 244 (9), 236 (23). **HRMS** (EI): calculated for $C_{35}H_{25}N_3$ ($[M]^+$) 487.20430, found 487.20439.

***N*,*N*-Dimethyl-5,13-di-*p*-tolylindolizino[6,5,4,3-*ija*]quinolino[2,3-*c*][1,6]naphthyridin-11-amine (5c).** According to modified general procedure B the title compound **5c** was obtained as a red solid in 21% yield (40 mg). **Mp** 272–277 °C; R_f 0.26 (heptane/ethyl acetate 2 : 1). **^{1}H NMR** (500 MHz, $CDCl_3$) δ = 8.73 (s, 1H), 8.05 (d, ^3J = 9.3 Hz, 1H), 8.03 (s, 1H), 7.90 (d, ^3J = 4.1 Hz, 1H), 7.70 (d, ^3J = 8.0 Hz, 2H), 7.47 (d, ^3J = 7.7 Hz, 2H), 7.40 (dd, ^3J = 9.3 Hz, ^4J = 2.8 Hz, 1H), 7.34 (d, ^3J = 7.7 Hz, 2H), 7.31 (d, ^3J = 8.0 Hz, 2H), 7.13 (s, 1H), 7.11 (d, ^3J = 4.1 Hz, 1H), 6.43 (d, ^4J = 2.8 Hz, 1H), 2.91 (s, 6H), 2.56 (s, 3H), 2.47 (s, 3H). **^{13}C NMR** (126 MHz, $CDCl_3$) δ = 147.9 (C), 144.9, 144.4 (CH), 143.6, 142.8, 141.4, 138.6, 138.4, 136.1, 135.0, 134.2, 134.1 (C), 130.9, 129.5, 129.4 (CH), 128.9 (C), 128.6 (CH), 128.5 (C), 128.0 (CH), 126.8 (C), 120.7 (CH), 119.9, 117.9, 117.3 (C), 114.6, 109.6, 106.8, 104.1 (CH), 40.5, 21.6, 21.3 (CH_3). **IR** (ATR, cm^{-1}): $\tilde{\nu}$ = 1613 (s), 1504 (m), 1440 (m), 1341 (m), 1055 (m), 892 (m), 814 (s), 800 (s), 781 (s), 587 (m), 495 (m). **MS** (EI, 70 eV): *m*/*z* (%) = 516 ($[M]^+$, 100), 501 (6), 500 (7), 486 (11), 472 (10), 471 (14), 400 (11), 258 (22), 257 (8). **HRMS** (EI): calculated for $C_{36}H_{28}N_4$ ($[M]^+$) 516.23085, found 516.23130.

11-Fluoro-5,13-di-*p*-tolylindolizino[6,5,4,3-*ija*]quinolino[2,3-*c*][1,6]naphthyridine (5d). According to general procedure B, the title compound **5d** was obtained as a red solid in 50% yield (87 mg). **Mp** 275–280 °C; R_f 0.37 (heptane/ethyl acetate 2 : 1). **^{1}H NMR** (300 MHz, $CDCl_3$) δ = 8.75 (s, 1H), 8.14–8.07 (m, 1H), 8.03 (s, 1H), 7.91 (d, ^3J = 4.2 Hz, 1H), 7.71–7.64 (m, 2H), 7.54–7.41 (m, 3H), 7.38–7.32 (m, 2H), 7.31–7.27 (m, 2H), 7.14 (s, 1H), 7.11–7.03 (m, 2H), 2.57 (s, 3H), 2.47 (s, 3H). **^{13}C NMR** (75 MHz, $CDCl_3$) δ = 160.0 (d, ^1J = 246.9 Hz, C), 145.7 (d, ^3J = 6.1 Hz, C), 145.1 (d, ^3J = 6.7 Hz, CH), 144.3 (d, ^4J = 2.6 Hz, C), 139.2, 138.8, 134.9, 134.7, 134.3, 134.0 (C), 131.1, 131.1, 131.0, 129.6 (CH), 129.2 (C), 128.5 (CH), 128.1 (C), 128.0 (CH), 126.0 (C), 120.7 (d, ^2J = 26.3 Hz, CH), 119.8, 117.7, 117.2 (C), 115.3, 111.1 (CH), 110.1 (d, ^2J = 23.8 Hz, CH), 107.1 (CH), 21.6, 21.3 (CH_3). **^{19}F NMR** (282 MHz, $CDCl_3$): δ = −113.0. **IR** (ATR, cm^{-1}): $\tilde{\nu}$ = 1735 (m), 1541 (m), 1457 (s), 1339 (m), 1230 (m), 1166 (s), 1041 (m), 822 (s), 800 (s), 734 (s), 600 (s), 490 (s). **MS** (EI, 70 eV): *m*/*z* (%) = 491 ($[M]^+$, 100), 490 (71), 489 (18), 487 (13), 476 (18), 475 (19), 245 (10), 238 (18), 237 (10). **HRMS** (EI): calculated for $C_{34}H_{22}N_3F$ ($[M]^+$) 491.17923, found 491.18050.

10,12-Difluor-5,13-di-*p*-tolylindolizino[6,5,4,3-*ija*]quinolino[2,3-*c*][1,6]naphthyridine (5e). According to general procedure B, the title compound **5e** was obtained as a red solid in 46% yield (78 mg). **Mp** 283–293 °C; R_f 0.30 (heptane/ethyl acetate 2 : 1). **^{1}H NMR** (300 MHz, $CDCl_3$) δ = 8.69 (s, 1H), 7.86 (d, ^3J = 4.2 Hz, 1H), 7.73 (s, 1H), 7.66–7.60 (m, 2H), 7.54–7.48 (m, 1H),7.47–7.41 (m, 2H), 7.36–7.30 (m, 4H), 7.12 (s, 1H), 7.02 (d, ^3J = 4.2 Hz, 1H), 6.83–6.73 (m, 1H), 2.56 (s, 3H), 2.47 (s, 3H). **^{13}C NMR** (126 MHz, $CDCl_3$) δ = 162.6 (dd, ^1J = 252.0 Hz, ^3J = 14.2 Hz, C), 159.8 (dd, ^1J = 264.4 Hz, ^3J = 14.4 Hz, C), 149.4 (dd, ^3J = 14.7 Hz, ^4J = 1.8 Hz, C), 146.0 (C), 145.3, 145.1 (CH), 144.7, 138.8 (C), 136.8 (d, ^4J = 4.4 Hz), 134.4, 134.0, 133.9 (C), 130.5 (CH), 129.7 (C), 129.6, 127.9 (CH), 127.3 (d, ^4J = 4.1 Hz, CH), 125.3, 119.6 (C), 117.9, 117.2 (C), 115.8 (CH), 114.7 (dd, ^3J = 6.1 Hz, ^3J = 2.0 Hz, C), 112.2 (CH), 108.6 (dd, ^2J = 20.1 Hz, ^4J = 4.9 Hz, CH), 107.3 (CH), 102.9 (pt, ^2J = 28.4 Hz, CH), 21.6, 21.3 (CH_3). **^{19}F NMR** (282 MHz, $CDCl_3$): δ = −106.5 (d, $^4J_{F,F}$ = 9.0 Hz), −99.9 (d, $^4J_{F,F}$ = 9.0 Hz). **IR** (ATR, cm^{-1}): $\tilde{\nu}$ = 1632 (s), 1543 (s), 1399 (m), 1339 (s), 1205 (s), 1135 (s), 1041 (m), 997 (m), 845 (s), 818 (s), 787 (s), 732 (s), 558 (s), 492 (m). **MS** (EI, 70 eV): *m*/*z* (%) = 509 ($[M]^+$, 100), 508 (84), 507 (12), 494 (21), 493 (29), 420 (6), 329 (7), 247 (13). **HRMS** (EI): calculated for $C_{34}H_{21}N_3F_2$ ($[M]^+$) 509.16981, found 509.17052.

9-Fluor-5,13-di-*p*-tolylindolizino[6,5,4,3-*ija*]quinolino[2,3-*c*][1,6]naphthyridine (5f). According to general procedure B, the title compound **5f** was obtained as an orange solid in 41% yield (67 mg). **Mp** 284–286 °C. R_f 0.28 (heptane/ethyl acetate 2 : 1); **^{1}H NMR** (500 MHz, $CDCl_3$) δ = 8.70 (s, 1H), 7.97 (d, ^3J = 4.2 Hz, 2H), 7.69–7.64 (m, 2H), 7.50 (d, ^3J = 7.7 Hz, 2H), 7.37–7.30 (m, 5H), 7.25–7.20 (m, 2H), 7.11 (s, 1H), 7.05 (d, ^3J = 4.1 Hz, 1H), 2.57 (s, 3H), 2.47 (s, 3H). **^{13}C NMR** (126 MHz, $CDCl_3$) δ = 157.3 (d, ^1J = 256.6 Hz, C), 146.3 (d, ^4J = 2.6 Hz, C), 145.1, 145.0 (CH), 144.8, 139.1, 138.8 (C), 138.5 (d, ^2J = 11.9 Hz, C), 135.1, 134.6, 134.2, 133.9 (C), 131.0, 129.6 (CH), 129.3 (C), 128.9 (d, ^5J = 1.7 Hz, C), 128.5, 128.0 (CH), 125.9 (C), 124.7 (d, ^3J = 7.8 Hz, CH), 122.7 (d, ^4J = 4.5 Hz, CH), 119.7, 117.9, 117.1 (C), 115.4 (CH), 113.9 (d, ^2J = 18.6 Hz, CH), 112.1, 107.3 (CH), 21.6, 21.3 (CH_3). **^{19}F NMR** (282 MHz, $CDCl_3$): δ = −126.0. **IR** (ATR, cm^{-1}): $\tilde{\nu}$ = 1537 (m), 1445 (m), 1339 (m), 1241 (m), 1119 (m), 1041 (m), 892 (m), 816 (s), 760 (s), 579 (m), 486 (m). **MS** (EI, 70 eV): *m*/*z* (%) = 491 ($[M]^+$, 100), 474 (9), 473 (45), 229 (1). **HRMS** (EI): calculated for $C_{34}H_{22}N_3F$ ($[M]^+$) 491.17923, found 491.17838.

5,15-Di-*p*-tolylbenzo[7,8]quinolino[2,3-*c*]indolizino[6,5,4,3-*ija*][1,6]naphthyridine (5h). According to general procedure B, the title compound **5h** was obtained as an orange solid in 41% yield (81 mg). **Mp** 334–339 °C; R_f 0.42 (heptane/ethyl acetate 2 : 1). **^{1}H NMR** (300 MHz, $CDCl_3$) δ = 9.47–9.43 (m, 1H), 8.65 (s, 1H), 7.99 (d, ^3J = 4.1 Hz, 1H), 7.90 (s, 1H), 7.76–7.70 (m, 1H), 7.70–7.60 (m, 4H), 7.51–7.41 (m, 3H), 7.37–7.27 (m, 4H),

7.25–7.21 (m, 1H), 7.08 (d, ^3J = 4.1 Hz, 1H), 7.07 (s, 1H), 2.58 (s, 3H), 2.47 (s, 3H). **^{13}C NMR** (75 MHz, $CDCl_3$) δ = 146.4, 145.8 (C), 144.1, 143.9 (CH), 143.2, 138.7, 138.6, 135.6, 134.8, 134.1, 134.0, 133.6 (C), 130.8 (CH), 130.7 (C), 129.5, 128.7 (CH), 128.6 (C), 128.0, 127.4, 126.8 (CH), 126.6 (C), 126.5, 125.2 (CH), 124.7 (C), 123.6 (CH), 119.9, 117.5, 117.1 (C), 115.1, 110.4, 106.9 (CH), 21.6, 21.3 (CH_3). **IR** (ATR, cm^{-1}): $\tilde{\nu}$ = 1533 (m), 1459 (m), 1356 (m), 1179 (m), 1111 (m), 1039 (m), 882 (m), 820 (s), 795 (s), 762 (s), 719 (m), 488 (m). **MS** (EI, 70 eV): *m*/*z* (%) = 523 ([M]$^+$, 100), 522 (44), 521 (15), 516 (10), 508 (12), 507 (14), 262 (14), 261 (13), 254 (19), 253 (11). **HRMS** (EI): calculated for $C_{38}H_{25}N_3$ ([M]$^+$) 523.20430, found 523.20496.

5,13-Diphenylindolizino[6,5,4,3-*ija*]quinolino[2,3-*c*][1,6]naphthyridine (5i). According to modified general procedure B ((1) *t* = 4 h; (2) *t* = 24 h), the title compound **5i** was obtained as an orange solid in 32% yield (57 mg); **Mp** 297–299 °C. R_f 0.43 (dcm/ethyl acetate 15 : 1). **^{1}H NMR** (300 MHz, $CDCl_3$) δ = 8.73 (s, 1H), 8.16–8.10 (m, 1H), 7.96–7.92 (m, 2H), 7.81–7.75 (m, 2H), 7.73–7.65 (m, 4H), 7.59–7.47 (m, 3H), 7.47–7.39 (m, 3H), 7.39–7.31 (m, 1H), 7.16 (s, 1H), 7.08 (d, ^3J = 4.2 Hz, 1H). **^{13}C NMR** (75 MHz, $CDCl_3$) δ = 148.1, 146.1 (C), 145.1, 145.0 (CH), 144.7, 138.3, 137.6, 134.3, 134.0 (C), 130.3, 130.2 (CH), 129.1 (C), 129.1, 128.9, 128.8, 128.7, 128.6, 128.1 (CH), 127.1 (C), 126.9 (CH), 126.2 (C), 125.8 (CH), 119.7, 117.4, 117.0 (C), 115.7, 111.3, 107.1 (CH). **IR** (ATR, cm^{-1}): $\tilde{\nu}$ = 1541 (m), 1337 (m), 1311 (m), 1183 (m), 1105 (m), 1034 (m), 888 (m), 849 (m), 808 (m), 760 (s), 701 (s), 649 (m), 474 (m). **MS** (EI, 70 eV): *m*/*z* (%) = 445 ([M]$^+$, 100), 444 (80), 443 (43), 442 (20), 441 (15), 418 (8), 367 (8), 223 (10), 222 (22), 221 (14), 207 (7). **HRMS** (ESI-TOF): calculated for $C_{32}H_{20}N_3$ ([M + H]$^+$) 446.1657, found 446.1656.

11-Fluor-5,13-diphenylindolizino[6,5,4,3-*ija*]quinolino[2,3-*c*][1,6]naphthyridine (5j). According to modified general procedure B ((2) 24 h reaction time) the title compound **5j** was obtained as an orange solid in 35% yield (56 mg); **Mp** 275–283 °C. R_f 0.33 (dcm/ethyl acetate 15 : 1). **^{1}H NMR** (300 MHz, $CDCl_3$) δ = 8.77 (s, 1H), 8.13 (dd, ^3J = 9.2 Hz, ^4J = 5.5 Hz, 1H), 7.94 (d, ^3J = 4.2 Hz, 1H), 7.82–7.76 (m, 2H), 7.73–7.66 (m, 3H), 7.59–7.47 (m, 4H), 7.46–7.39 (m, 3H), 7.18 (s, 1H), 7.10 (d, ^3J = 4.2 Hz, 1H), 7.07–7.01 (m, 1H). **^{13}C NMR** (75 MHz, $CDCl_3$/TFA) δ = 162.1 (d, ^1J = 257.8 Hz, C), 158.2 (d, ^4J = 5.8 Hz, C), 139.7 (C), 138.5 (CH), 137.6 (d, ^4J = 2.0 Hz, C), 137.1, 135.2, 134.9 (C), 134.8 (CH), 134.1, 133.5 (C), 132.4, 131.1, 129.8 (CH), 128.7 (d, ^3J = 8.7 Hz, C), 128.5 (d, ^2J = 25.6 Hz, CH), 128.3, 126.7 (CH), 122.5 (C), 122.4 (d, ^3J = 9.3 Hz, CH), 120.5, 118.6 (CH), 118.6, 118.3, 116.3 (C), 114.6 (CH), 113.1 (d, ^2J = 25.1 Hz, CH). **^{19}F NMR** (282 MHz, $CDCl_3$): δ = −112.8. **IR** (ATR, cm^{-1}): $\tilde{\nu}$ = 1539 (m), 1459 (m), 1434 (m), 1356 (m), 1232 (m), 1175 (m), 1107 (m), 828 (m), 800 (m), 725 (m), 696 (s), 604 (m), 565 (m), 474 (m). **MS** (EI, 70 eV): *m*/*z* (%) = 463 ([M]$^+$, 100), 462 (78), 461 (43), 460 (13), 459 (13), 436 (5), 385 (9), 232 (11), 231 (26), 230 (12), 217 (5). **HRMS** (ESI-TOF): calculated for $C_{32}H_{19}FN_3$ ([M + H]$^+$) 464.1563, found 464.1554.

4,4′-(11-Fluorindolizino[6,5,4,3-*ija*]quinolino[2,3-*c*][1,6]naphthyridine-5,13-diyl)bis(*N*,*N*-dimethylaniline) (5k). According to modified general procedure B ((2) 8 h reaction time) the title compound **5k** was obtained as an orange solid in 39% yield (95 mg); **mp** 301–305 °C. R_f 0.34 (dcm/ethyl acetate 3 : 1). **^{1}H NMR** (500 MHz, $CDCl_3$) δ = 8.76 (s, 1H), 8.21 (s, 1H), 8.14 (dd, ^3J = 9.2 Hz, ^4J = 5.5 Hz, 1H), 7.95 (d, ^3J = 4.1 Hz, 1H), 7.73–7.68 (m, 2H), 7.51–7.46 (m, 1H), 7.27–7.23 (m, 1H), 7.22–7.19 (m, 2H), 7.17 (d, ^3J = 4.1 Hz, 1H), 7.14 (s, 1H), 6.99–6.95 (m, 2H), 6.89–6.86 (m, 2H), 3.12 (s, 6H), 3.06 (s, 6H). **^{13}C NMR** (126 MHz, $CDCl_3$) δ = 160.0 (d, ^1J = 246.4 Hz, C), 150.8, 150.7 (C), 146.6 (d, ^4J = 6.0 Hz, C), 145.3 (C), 145.1, 144.7 (CH), 144.6 (d, ^4J = 2.4 Hz, C), 134.4, 133.9 (C), 130.9 (d, ^3J = 8.9 Hz, CH), 129.5 (C), 129.4, 128.9 (CH), 128.8 (d, ^3J = 9.2 Hz, C), 126.0, 125.4, 124.8 (C), 120.5 (d, ^2J = 26.5 Hz, CH), 120.1, 118.3, 117.5 (C), 114.0, 113.5, 112.3, 110.9 (CH), 110.4 (d, ^2J = 23.5 Hz, CH), 107.2 (CH), 40.4, 40.3 (CH_3). **^{19}F NMR** (282 MHz, $CDCl_3$): δ = −113.6. **IR** (ATR, cm^{-1}): $\tilde{\nu}$ = 1607 (s), 1523 (s), 1508 (s), 1428 (m), 1360 (s), 1335 (s), 1230 (m), 1191 (s), 1164 (s), 816 (s), 804 (s), 793 (s), 729 (m), 600 (m). **MS** (EI, 70 eV): *m*/*z* (%) = 550 ([M]$^+$, 62), 549 (100), 548 (19), 535 (15), 534 (32), 520 (15), 518 (11), 479 (19), 274 (18), 252 (12). **HRMS** (EI): calculated for $C_{36}H_{28}FN_5$ ([M]$^+$) 550.2407, found 550.2407.

11-Fluor-5,13-bis(4-fluorphenyl)indolizino[6,5,4,3-*ija*]quinolino[2,3-*c*][1,6]naphthyridine (5l). According to modified general procedure B ((2) 24 h reaction time) the title compound **5l** was obtained as a yellow solid in 65% yield (119 mg); **mp** 318–323 °C. R_f 0.50 (dcm/ethyl acetate 15 : 1). **^{1}H NMR** (300 MHz, $CDCl_3$) δ = 9.40 (s, 1H), 8.77 (d, ^3J = 4.7 Hz, 1H), 8.51 (dd, ^3J = 9.4 Hz, ^4J = 4.5 Hz, 1H), 8.05–7.97 (m, 2H), 7.84 (s, 1H), 7.82–7.75 (m, 2H), 7.71 (d, ^3J = 4.7 Hz, 1H), 7.64–7.56 (m, 2H), 7.50–7.43 (m, 2H), 7.40–7.31 (m, 3H). **^{13}C NMR** (75 MHz, $CDCl_3$) δ = 164.7 (d, ^1J = 256.9 Hz, C), 164.3 (d, ^1J = 252.6 Hz, C), 162.0 (d, ^1J = 258.1 Hz, C), 156.7 (d, ^4J = 5.8 Hz, C), 138.8 (CH), 138.2 (C), 137.4 (d, ^4J = 2.0 Hz, C), 137.0, 135.2 (C), 134.7 (CH), 134.4 (C), 130.2 (d, ^3J = 8.8 Hz, CH), 130.2 (C), 129.2 (d, ^3J = 8.3 Hz. CH), 129.1 (d, ^4J = 4.2 Hz, C), 128.7 (d, ^3J = 9.8 Hz, C), 128.4 (d, ^2J = 26.7 Hz, CH), 122.7 (d, ^3J = 9.2 Hz, CH), 122.3 (C), 120.8 (CH), 119.9 (d, ^2J = 22.3 Hz, CH), 118.6 (CH), 118.3, 118.3 (C), 117.0 (d, ^2J = 22.1 Hz, CH), 116.5 (C), 114.3 (CH), 112.7 (d, ^2J = 24.9 Hz, CH). **^{19}F NMR** (282 MHz, $CDCl_3$): δ = −102.9, −105.2, −108.5. **IR** (ATR, cm^{-1}): $\tilde{\nu}$ = 1502 (s), 1461 (m), 1339 (m), 1224 (s), 1158 (m), 828 (s), 802 (s), 779 (m), 725 (m), 587 (m), 560 (s), 540 (s), 505 (s). **MS** (EI, 70 eV): *m*/*z* (%) = 499 ([M]$^+$, 100), 498 (61), 497 (31), 459 (43), 458 (86), 457 (13), 250 (44), 249 (20), 248 (17), 239 (18), 229 (24). **HRMS** (ESI-TOF): calculated for $C_{32}H_{17}F_3N_3$ ([M + H]$^+$) 500.1375, found 500.1377.

Conflicts of interest

There are no conflicts to declare.

Acknowledgements

Financial support by the State of Mecklenburg-Vorpommern is gratefully acknowledged.

References

1 H. Balli and M. Zeller, Neue Heteroarene: Synthese und spektrale Daten von Indolizino[6,5,4,3-aij]chinolin («Ullazin») und einigen Derivaten, *Helv. Chim. Acta*, 1983, **66**, 2135–2139.

2 J. H. Delcamp, A. Yella, T. W. Holcombe, M. K. Nazeeruddin and M. Grätzel, The molecular engineering of organic sensitizers for solar-cell applications, *Angew. Chem., Int. Ed.*, 2013, **52**, 376–380.

3 (*a*) J. Feng, Y. Jiao, W. Ma, M. K. Nazeeruddin, M. Grätzel and S. Meng, First Principles Design of Dye Molecules with Ullazine Donor for Dye Sensitized Solar Cells, *J. Phys. Chem. C*, 2013, **117**, 3772–3778; (*b*) Q. Le Bao, S. Thogiti, G. Koyyada and J. H. Kim, Synthesis and photovoltaic performance of novel ullazine-based organic dyes for dye-sensitized solar cells, *Jpn. J. Appl. Phys.*, 2019, **58**, 12011; (*c*) C. Cebrián, Ullazine-based materials: towards novel opportunities in organic electronics, *J. Mater. Chem. C*, 2018, **6**, 11943–11950.

4 (*a*) Q. Ge, B. Li and B. Wang, Synthesis of substituted benzoijimidazo-2,1,5-dequinolizine by rhodium(III)-catalyzed multiple C-H activation and annulations, *Org. Biomol. Chem.*, 2016, **14**, 1814–1821; (*b*) Y. Guo, L. Zhang, C. Li, M. Jin, Y. Zhang, J. Ye, Y. Chen, X. Wu and X. Liu, BN/BO-Ullazines and Bis-BO-Ullazines: Effect of BO Doping on Aromaticity and Optoelectronic Properties, *J. Org. Chem.*, 2021, **86**, 12507–12516; (*c*) C. Li, Y. Liu, Z. Sun, J. Zhang, M. Liu, C. Zhang, Q. Zhang, H. Wang and X. Liu, Synthesis, Characterization, and Properties of Bis-BN Ullazines, *Org. Lett.*, 2018, **20**, 2806–2810; (*d*) P. Pierrat, S. Hesse, C. Cebrián and P. C. Gros, Controlling charge-transfer properties through a microwave-assisted mono- or bis-annulation of dialkynyl-N-(het)arylpyrroles, *Org. Biomol. Chem.*, 2017, **15**, 8568–8575; (*e*) S. Janke, S. Boldt, P. Nakielski, A. Villinger, P. Ehlers and P. Langer, Synthesis and Properties of 5-Azaullazines, *J. Org. Chem.*, 2023, **88**, 10470–10482.

5 S. Boldt, S. Parpart, A. Villinger, P. Ehlers and P. Langer, Synthesis and Properties of Aza-ullazines, *Angew. Chem., Int. Ed.*, 2017, **56**, 4575–4578.

6 (*a*) G. Zhang, P. Gautam and J. M. W. Chan, Symmetrical and unsymmetrical fluorine-rich ullazines via controlled cycloaromatizations, *Org. Chem. Front.*, 2020, **7**, 787–795; (*b*) H. Qiao, Y. Deng, R. Peng, G. Wang, J. Yuan and S. Tan, Effect of π-spacers and anchoring groups on the photovoltaic performances of ullazine-based dyes, *RSC Adv.*, 2016, **6**, 70046–70055; (*c*) D. Wan, X. Li, R. Jiang, B. Feng, J. Lan, R. Wang and J. You, Palladium-Catalyzed Annulation of Internal Alkynes: Direct Access to π-Conjugated Ullazines, *Org. Lett.*, 2016, **18**, 2876–2879; (*d*) S. Mathew, N. A. Astani, B. F. E. Curchod, J. H. Delcamp, M. Marszalek, J. Frey, U. Rothlisberger, M. K. Nazeeruddin and M. Grätzel, Synthesis, characterization and ab initio investigation of a panchromatic ullazine–porphyrin photosensitizer for dye-sensitized solar cells, *J. Mater. Chem. A*, 2016, **4**, 2332–2339; (*e*) K. Kanno, Y. Liu, A. Iesato, K. Nakajima and T. Takahashi, Chromium-mediated synthesis of polycyclic aromatic compounds from halobiaryls, *Org. Lett.*, 2005, **7**, 5453–5456.

7 (*a*) E. S. Larsen, G. Ahumada, P. R. Sultane and C. W. Bielawski, Stereoelectronically-induced allosteric binding: shape complementarity promotes positive cooperativity in fullerene/buckybowl complexes, *Chem. Commun.*, 2022, **58**, 6498–6501; (*b*) S. Li, Y. Sun, X. Li, O. Smaga, S. Koniarz, M. Stępień and P. J. Chmielewski, 1,3-Dipolar cycloaddition of polycyclic azomethine ylide to norcorroles: towards dibenzoullazine-fused derivatives, *Chem. Commun.*, 2022, **58**, 6510–6513.

8 J. Zhou, W. Yang, B. Wang and H. Ren, Friedel-Crafts arylation for the formation of $C(sp^2)$–$C(sp^2)$ bonds: a route to unsymmetrical and functionalized polycyclic aromatic hydrocarbons from aryl triazenes, *Angew. Chem., Int. Ed.*, 2012, **51**, 12293–12297.

9 D. Wang, Y. Liu, L. Wang, H. Cheng, Y. Zhang and G. Gao, Synthesis of π-extended dibenzo[d,k]ullazines by a palladium-catalyzed double annulation using arynes, *Chin. Chem. Lett.*, 2021, **32**, 1407–1410.

10 R. Berger, M. Wagner, X. Feng and K. Müllen, Polycyclic aromatic azomethine ylides: a unique entry to extended polycyclic heteroaromatics, *Chem. Sci.*, 2015, **6**, 436–441.

11 S. Ito, Y. Tokimaru and K. Nozaki, Isoquinolino[4,3,2-de]phenanthridine: synthesis and its use in 1,3-dipolar cycloadditions to form nitrogen-containing polyaromatic hydrocarbons, *Chem. Commun.*, 2015, **51**, 221–224.

12 M. Richter, M. Borkowski, Y. Fu, E. Dmitrieva, A. Popov, J. Ma, T. Marszalek, W. Pisula and X. Feng, Synthesis and Self-Assembly Behavior of Double Ullazine-Based Polycyclic Aromatic Hydrocarbons, *Org. Mater.*, 2021, **03**, 198–203.

13 S. Ito, Y. Tokimaru and K. Nozaki, Benzene-Fused Azacorannulene Bearing an Internal Nitrogen Atom, *Angew. Chem., Int. Ed.*, 2015, **54**, 7256–7260.

14 J. Hager, S. Kang, P. J. Chmielewski, T. Lis, D. Kim and M. Stępień, Acenaphthylene-fused ullazines: fluorescent π-extended monopyrroles with tunable electronic gaps, *Org. Chem. Front.*, 2022, **9**, 3179–3185.

15 D. Miao, C. Aumaitre and J.-F. Morin, Photochemical synthesis of π-extended ullazine derivatives as new electron donors for efficient conjugated D–A polymers, *J. Mater. Chem. C*, 2019, **7**, 3015–3024.

16 L. S. Povarov, α,β-Unsaturated Ethers and their analogues in reactions of diene synthesis, *Russ. Chem. Rev.*, 1967, **36**, 656–670.

17 (*a*) J. Clerigué, M. T. Ramos and J. C. Menéndez, Enantioselective catalytic Povarov reactions, *Org. Biomol. Chem.*, 2022, **20**, 1550–1581; (*b*) E. A. Kuznetsova, A. V. Smolobochkin, T. S. Rizbayeva, A. S. Gazizov, J. K. Voronina, O. A. Lodochnikova, D. P. Gerasimova, A. B. Dobrynin, V. V. Syakaev, D. N. Shurpik, I. I. Stoikov, A. R. Burilov, M. A. Pudovik and O. G. Sinyashin, Diastereoselective intramolecular cyclization/Povarov reaction cascade for the one-pot synthesis of polycyclic quinolines, *Org. Biomol. Chem.*, 2022, **20**, 5515–5519.

18 B. Chakraborty, A. Kar, R. Chanda and U. Jana, Application of the Povarov Reaction in Biaryls under Iron Catalysis for the General Synthesis of Dibenzo[a,c]Acridines, *J. Org. Chem.*, 2020, **85**, 9281–9289.

19 F. Spruner von Mertz, R. Molenda, S. Boldt, A. Villinger, P. Ehlers and P. Langer, Synthesis and Properties of Diphenylbenzo[j]naphtho[2,1,8-def][2,7]phenanthrolines, *Chem. – Eur. J.*, 2023, **29**, e202204011.

20 R. Molenda, S. Boldt, A. Villinger, P. Ehlers and P. Langer, Synthesis of 2-Azapyrenes and Their Photophysical and Electrochemical Properties, *J. Org. Chem.*, 2020, **85**, 12823–12842.

21 S. Parpart, S. Boldt, P. Ehlers and P. Langer, Synthesis of Unsymmetrical Aza-Ullazines by Intramolecular Alkynyl-Carbonyl Metathesis, *Org. Lett.*, 2018, **20**, 122–125.

22 A. M. Brouwer, Standards for photoluminescence quantum yield measurements in solution (IUPAC Technical Report), *Pure Appl. Chem.*, 2011, **83**, 2213–2228.

23 M. J. Frisch, G. W. Trucks, H. B. Schlegel, G. E. Scuseria, M. A. Robb, J. R. Cheeseman, G. Scalmani, V. Barone, G. A. Petersson, H. Nakatsuji, X. Li, M. Caricato, A. V. Marenich, J. Bloino, B. G. Janesko, R. Gomperts, B. Mennucci, H. P. Hratchian, J. V. Ortiz, A. F. Izmaylov, J. L. Sonnenberg, J. Williams, F. Ding, F. Lipparini, F. Egidi, J. Goings, B. Peng, A. Petrone, T. Henderson, D. Ranasinghe, V. G. Zakrzewski, J. Gao, N. Rega, G. Zheng, W. Liang, M. Hada, M. Ehara, K. Toyota, R. Fukuda, J. Hasegawa, M. Ishida, T. Nakajima, Y. Honda, O. Kitao, H. Nakai, T. Vreven, K. Throssell, J. A. Montgomery Jr., J. E. Peralta, F. Ogliaro, M. J. Bearpark, J. J. Heyd, E. N. Brothers, K. N. Kudin, V. N. Staroverov, T. A. Keith, R. Kobayashi, J. Normand, K. Raghavachari, A. P. Rendell, J. C. Burant, S. S. Iyengar, J. Tomasi, M. Cossi, J. M. Millam, M. Klene, C. Adamo, R. Cammi, J. W. Ochterski, R. L. Martin, K. Morokuma, O. Farkas, J. B. Foresman and D. J. Fox, *Gaussian 16 Rev. C.01*, Wallingford, CT, 2016.

24 (*a*) D. Bischof, M. W. Tripp, P. E. Hofmann, C.-H. Ip, S. I. Ivlev, M. Gerhard, U. Koert and G. Witte, Regioselective Fluorination of Acenes: Tailoring of Molecular Electronic Levels and Solid-State Properties, *Chem. – Eur. J.*, 2022, **28**, e202103653; (*b*) J. Holec, B. Cogliati, J. Lawrence, A. Berdonces-Layunta, P. Herrero, Y. Nagata, M. Banasiewicz, B. Kozankiewicz, M. Corso, D. G. de Oteyza, A. Jancarik and A. Gourdon, A Large Starphene Comprising Pentacene Branches, *Angew. Chem., Int. Ed.*, 2021, **60**, 7752–7758; (*c*) O. Francesconi, M. Martinucci, L. Badii, C. Nativi and S. Roelens, A Biomimetic Synthetic Receptor Selectively Recognising Fucose in Water, *Chem. – Eur. J.*, 2018, **24**, 6828–6836.

25 M.-L. Tan, S. Tong, S.-K. Hou, J. You and M.-X. Wang, Copper-Catalyzed N,N-Diarylation, of Amides for the Construction of 9,10-Dihydroacridine Structure and Applications in the Synthesis of Diverse Nitrogen-Embedded Polyacenes, *Org. Lett.*, 2020, **22**, 5417–5422.

26 J. Liu, C. Chen and C. Fang, Polarity-Dependent Twisted Intramolecular Charge Transfer in Diethylamino Coumarin Revealed by Ultrafast Spectroscopy, *Chemosensors*, 2022, **10**, 411.

27 P. v. R. Schleyer, C. Maerker, A. Dransfeld, H. Jiao and N. J. R. van Eikema Hommes, Nucleus-Independent Chemical Shifts: A Simple and Efficient Aromaticity Probe, *J. Am. Chem. Soc.*, 1996, **118**, 6317–6318.

28 E. Paenurk and R. Gershoni-Poranne, Simple and efficient visualization of aromaticity: bond currents calculated from NICS values, *Phys. Chem. Chem. Phys.*, 2022, **24**, 8631–8644.